Expanding generality of surface-enhanced Raman spectroscopy with borrowing SERS activity strategy

Zhong-Qun Tian,* Bin Ren,* Jian-Feng Li and Zhi-Lin Yang

Received (in Cambridge, UK) 21st November 2006, Accepted 9th March 2007
First published as an Advance Article on the web 4th April 2007
DOI: 10.1039/b616986d

Surface-enhanced Raman scattering (SERS) was discovered three decades ago and has gone through a tortuous pathway to develop into a powerful diagnostic technique. Recently, the lack of substrate, surface and molecular generalities of SERS has been circumvented to a large extent by devising and utilizing various nanostructures by many groups including ours. This article aims to present our recent approaches of utilizing the borrowing SERS activity strategy mainly through constructing two types of nanostructures. The first nanostructure is chemically synthesized Au nanoparticles coated with ultra-thin shells (*ca.* one to ten atomic layers) of various transition metals, *e.g.*, Pt, Pd, Ni and Co, respectively. Boosted by the long-range effect of the enhanced electromagnetic (EM) field generated by the highly SERS-active Au core, the originally low surface enhancement of the transition metal can be substantially improved giving total enhancement factors up to 10^4–10^5. It allows us to obtain the Raman spectra of surface water, having small Raman cross-section, on several transition metals for the first time. To expand the surface generality of SERS, tip-enhanced Raman spectroscopy (TERS) has been employed. With TERS, a nanogap can be formed controllably between an atomically flat metal surface and the tip with an optimized shape, within which the enhanced EM field from the tip can be coupled (borrowed) effectively. Therefore, one can obtain surface Raman signals (TERS signals) from adsorbed species at Au(110), Au(111) and, more importantly, Pt(110) surfaces. The enhancement factor achieved on these single crystal surfaces can be up to 10^6, especially with a very high spatial resolution down to about 14 nm. To fully accomplish the borrowing strategy from different nanostructures and to explain the experimental observations, a three-dimensional finite-difference time-domain method was used to calculate and evaluate the local EM field on the core–shell nanoparticle surfaces and the TERS tips. Finally, prospects and further developments of this valuable strategy are briefly discussed with emphasis on the emerging experimental methodologies.

Introduction

Generality of surface Raman spectroscopy

Two years after the report of "a new type of secondary radiation" from the scattering of focused beams of sunlight in benzene liquid,[1] Sir. C. V. Raman received the Nobel Prize in Physics "for his work on the scattering of light and for the discovery of the effect named after him".[2] Such a great honor was awarded soon because the scientific community immediately recognized the great value of the Raman effect that can be developed into a powerful fingerprint vibrational spectroscopy in qualitative and quantitative analysis. However, Raman scattering is a two-photon process occurring at a time scale of *ca.* 10^{-12} s and the cross section of a molecule for such a process is about 10^6 and 10^{14} times smaller than those of infrared and fluorescence processes, respectively.[3] Therefore, Raman spectroscopy has an intrinsically low detection sensitivity. Subsequently, the development of this promising technique to a powerful and widely used tool had been slow and tortuous and it had taken Raman spectroscopy more than three decades to be recognized as a widely used technique. This detection sensitivity was significantly improved in the early 1960s when the laser was invented and then used as an ultra-intense light source for Raman spectroscopy. The use of lasers in the ultraviolet (UV) through to the near-IR makes Raman spectroscopy a flexible technique that can analyze samples from lunar rocks to ocean ore, from silicon chips to plastic, and from proteins to drugs at the molecular level.[4–9]

In 1970s, the potential application in the fields of surface science and trace analysis seemed to be the only challenging issue related to the generality of Raman spectroscopy. In these two fields, the number of probe molecules, ranging from about 10 million down to one, is substantially smaller than that of bulk materials or solution in the normal Raman measurements. The following equation gives the Raman intensity expression for a vibrational mode of a molecule based on Placzek's polarizability theory with regard to the instrumental and surface factors:[10]

$$I_{mn} = \frac{2^7\pi^5}{3^2c^4} I_0(\nu_0 - \nu_{mn})^4 \sum_{\rho\sigma} \left|(\alpha_{\rho\sigma})mn\right|^2 NA\Omega QT_0T_m \quad (1)$$

State Key Laboratory for Physical Chemistry of Solid Surfaces and Department of Chemistry, College of Chemistry and Chemical Engineering, Xiamen University, Xiamen, 361005, China. E-mail: zqtian@xmu.edu.cn; bren@xmu.edu.cn; Fax: +86-592-2183407; Tel: +86-592-2186979

where N is the number density of the adsorbate (molecules cm^{-2}), A is the surface area illuminated by the laser beam (cm^2), Ω is the solid angle of the collection optics (sr), QT_mT_0 is the product of the detector efficiency, the throughput of the dispersion system and the transmittance of the collection optics. Even if the probe molecules fully cover a flat surface, the number of molecules is only about 10^7 within the laser spot of about 1 μm in diameter. Considering that typically one Raman photon is produced by about 10^{10} incident photons, it is still not sufficient to detect a surface adsorbate with monolayer coverage nowadays even with state-of-the-art Raman instruments through the improvement on ΩQT_mT_0.[3,4] Although the surface Raman scattering intensity scales linearly with the incident laser power (I_0) and the fourth power of energy (v_0), the ultimate sensitivity is limited by the surface damage threshold of the substrate. An alternative way to increase the intensity is to increase the sample concentration. This approach is effective for studying the bulk signal from a liquid phase and transparent samples, but has limitation for the study of surface adsorption, where normally only one monolayer of molecules are presented, and the signal for almost all non-resonant adsorbates at this concentration level is below the detection limit. As a consequence of the inherent weakness of the scattering mechanism, Raman spectroscopy had seldom been utilized for characterizing surface species before the mid-1970s.[11–13]

However, Raman spectroscopy is highly attractive to surface scientists as it can in principle provide much insight into a variety of chemical, physical and biological surfaces and interfaces at the molecular level, *e.g.*, determining surface bonding, molecular conformation and adsorption orientation. It can be applied to *in-situ* investigation of solid–liquid, solid–gas and solid–solid interfaces and processes, to which many surface techniques are not applicable. These important advantages have led researchers to seek every possible way to improve the generality of Raman spectroscopy in surface science and related fields, *i.e.*, to establish surface Raman spectroscopy.

The landmark breakthrough in the field of surface Raman spectroscopy started in mid-1970s. The first measurement of potential-dependent surface Raman spectra from pyridine

Zhong-Qun Tian

Zhong-Qun Tian received his BSc at Xiamen University in 1982. He moved to University of Southampton in 1983 and worked on surface-enhanced Raman spectroscopic studies on electrochemical deposition and adsorption with Prof. Martin Fleischmann. After obtaining his PhD in 1987 he returned to Xiamen University. He was promoted to full professor in 1992 and serves as the director of State Key Laboratory for Physical Chemistry of Solid Surfaces from 2003. He is a Member of Chinese Academy of Sciences and Fellow of the Royal Society of Chemistry, Titular Member of Division of Physical and Biophysical Chemistry in IUPAC, and member of advisory board of four international journals. His main research interests are surface-enhanced Raman spectroscopy, spectro-electrochemistry and nano-electrochemistry.

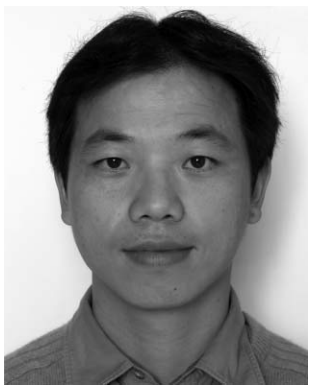

Bin Ren

Bin Ren obtained his PhD in Physical Chemistry in 1998 with Prof. Zhong-Qun Tian at Xiamen University on developing methodologies for extending SERS to transition-metal surfaces. He is now a full professor at the same university and a permanent research scientist in the State Key Laboratory for Physical Chem?istry of Solid Surfaces. He was supported by Alexander von Humboldt Foundation to conduct research on tip-enhanced Raman spectroscopy at the Fritz-Haber Institute in Germany with Dr Pettinger as an AvH fellow on his sabbatical leave in 2003. He won the Chinese Young Chemists Award in 2004. His research interest is on TERS, in-situ electrochemical SERS, spectro-, and interfacial-electrochemistry.

Jian-Feng Li

Jian-Feng Li obtained his BSc at Zhejiang University in 2003 and is now pursuing his PhD degree with Prof. Zhong-Qun Tian at Xiamen University. His thesis is concentrated on the synthesis of various types of core–shell nanoparticles that are used as non-traditional SERS substrates for detecting systems with very weak Raman signal.

Zhi-Lin Yang

Zhi-Lin Yang received his PhD degree in Physical Chemistry in 2006 at Xiamen University under supervision of Professor Zhong-Qun Tian, working on the optical properties of metallic nanoparticles and the electromagnetic field enhancement of surface-enhanced Raman scattering. He is now an associate professor in the Department of Physics at Xiamen University. His present research interest is on the theoretical modeling of nano-optics and plasmonics.

adsorbed on an electrochemically roughened silver electrode was reported by Fleischmann, Hendra and McQuillan.[14] The Raman spectra proved to be of very high quality and evidently was due to a surface species in view of its electrode potential dependency. In retrospect, this was, in fact, the first SERS measurement although it was not recognized as such at the time. The authors initially thought that the electrochemical roughening procedure had significantly increased the surface area of the electrode and therefore the number of surface molecules so that the intense surface Raman signal of pyridine, a molecule with very large Raman cross section, can be obtained, according to eqn (1). After carefully making the calculation and experiment, Van Duyne and co-workers realized that the major contribution to the intense Raman signal is due to an anomalous enhancement of 10^5–10^6 times compared to the intensities predicted from the scattering cross-section for the bulk pyridine. However, their paper was rejected several times as the so-called surface enhancement was not believed. In 1977 Jeanmaire and Van Duyne eventually published their paper,[15] and independently Albrecht and Creighton reported a similar result.[16] They provided strong evidences to demonstrate that the enormously strong surface Raman signal must be caused by a true enhancement of the Raman scattering efficiency itself. The effect was later called surface-enhanced Raman scattering (SERS).[17]

The discovery of SERS impacted on surface science and spectroscopy because the intrinsically low detection sensitivity is no longer a fatal disadvantage for surface Raman spectroscopy. Surface-enhanced Raman spectroscopy (SERS) offers a means to overcome the dual obstacles of sensitivity and surface selectivity, allowing the obtainment of surface vibrational data *in situ* even in electrochemical environments. Vigorous research activities have ensued not only in the electrochemical environment but also in air and under UHV conditions on virtually every conceivable metal surface substrates, colloids, powders, and even catalysts supported on insulator granules.[18–26] More importantly, the effect makes it possible to use SERS as an *in situ* diagnostic probe for determining the detailed molecular structure and orientation of surface species, which is widely applicable to electrochemical, biological and other ambient interfaces.[18–26]

Substrate, surface and molecule generalities of SERS

The upsurge of optimism that the surface generality of Raman spectroscopy achieved after the discovery of SERS was unfortunately quite short and then calmed down in the late-1970s. It turned out that only a few 'free-electron-like' metals, mainly Ag, Au and Cu, provide a large SERS effect under the condition that the metal surface roughness or the colloid size must be at the scale of several tens of nanometers. Two key stumbling blocks in applying SERS were perceived to be lack of substrate generality and surface generality. The former severely limited the breadth of practical applications for SERS in various materials widely used in electrochemistry, corrosion, catalysis and other industries. The latter confined SERS studies to surfaces with ill-defined morphology that is not commonly acceptable in the community of surface science.

In the 1980s and early 1990s many groups had made great efforts to break these two key limitations, which were to generate SERS activity from metallic surfaces other than Ag, Cu and Au and to obtain Raman signals from atomically flat (single crystal) surfaces. Some of them claimed that they have obtained unenhanced[27–29] and enhanced[30,31] Raman signals from adsorbates on either roughened or mechanically polished Pt and Rh electrodes, or porous Ni, Pd, Pt, Ti and Co films.[32] However, some of the reported SERS spectra could either not be repeated or barely detected. Therefore, these efforts were not recognized by the communities of Raman spectroscopy and surface science, pointing to a gloomy future in this direction. As a consequence of lack of the substrate and surface generalities and the difficulty to comprehensively elucidate the SERS mechanism, many research groups gradually left the field, leading to a low tide from 1980s to the mid-1990s.

Boosted by the rapid development of nanoscience in the 1990s, SERS has attracted a wide interest again since about 1996 and achieved a second upsurge in the 2000s.[33–36] Recalling the development of science during this period, we will find that the renaissance of SERS is not out of expectation as SERS is in fact one of the important branches of the ascendant nanotechnology. It has been found that SERS activity is critically dependent on the size, shape and aggregation of nanoparticles. A great variety of techniques of nanoscience have been employed to synthesize and characterize SERS-related nanoparticles or nanostructures in a well controllable state, which is essentially important to develop SERS. Such efforts have led to a most significant progress in this field, *i.e.*, bringing SERS into the forefront with single-molecular Raman spectroscopy.[37–40] High-quality SERS or surface-enhanced resonance Raman scattering (SERRS) spectra from a single molecule adsorbed on well-characterized silver and gold nanoparticles have been obtained, with an extraordinary signal enhancement up to 10^{14}, which is much higher than the widely accepted value of 10^6 for SERS. The high quality single-molecular SERS spectra have improved the molecule generality and marked SERS as one of the most promising tools for trace analysis in life and medical sciences as well as security and environment protection with single molecule sensitivity.[41]

In parallel to the achievement with single-molecular sensitivity, the substrate generality of SERS has also been substantially improved. It has been demonstrated that SERS could be generated directly on electrode surfaces made from massive transition metals and their alloys.[42–44] This advance was made possible primarily owing to the development of various methods for fabricating nanostructured surfaces and the application of the confocal microscope and the holographic notch filter in Raman instruments.[45] The Raman measurements, which conventionally employed high-dispersion double or triple monochromators to filter out the elastically scattered laser radiation, can now be performed with a single spectrograph instrument equipped with a holographic notch filter. The throughput of a single-grating system is far higher than, for example, a triple monochromator. These new developments have resulted in unprecedented sensitivity of Raman spectroscopy. The improvement in the Raman instrument alone is still not sufficient to obtain surface Raman

signals from transition-metal (hereafter designated as TM) surfaces, which becomes possible only after substrates with SERS activity have been successfully obtained. In the past 10 years, we have employed and developed five SERS activation procedures for different transition metals, *i.e.*, potential-controlled oxidation and reduction cycles(s) (ORC),[46] current-controlled ORC,[47] chemical etching,[48] electrodeposition,[49] and template synthesis.[50] We have obtained good-quality surface Raman signals from bare Pt, Pd, Ru, Rh, Fe, Co and Ni electrodes and demonstrated that they exhibit a surface enhancement ranging from one to three orders of magnitude.[43,44,51] The severe limitation encountered in substrate generality of SERS appears to be partially overcome.

After obtaining SERS from TM systems, naturally, we have tried to figure out microscopically the origin of SERS from transition metals that had not been considered as effective SERS substrates. In general, as the major contribution to SERS, the electromagnetic field enhancement is determined by the interaction of (incident and scattered) light and metal, generating surface plasmon resonance at metal nanoparticles or surface nanostructures. The electromagnetic field of the light at the surface can be greatly enhanced under conditions of surface plasmon resonance (collective electron resonance) for 'free-electron' metals.[18,35,52–56] The conduction electrons in these nanoparticles can be driven effectively by visible light to oscillate collectively, generating a strong electromagnetic field near the surface of metal nanoparticles. To meet the conditions of good surface plasmon resonance, the metal usually should have a small value of the imaginary component of the dielectric constant. This is impossible for a TM because in the visible light region the values of the imaginary part of dielectric constants is large and the interband excitation occurs as the Fermi level locates at the d band.[57] The coupling between conduction electrons and interband electronic transitions depresses considerably the quality of the surface plasmon resonance of TMs.[58] Accordingly, the SERS activity of electrochemically roughened TM surfaces is in general quite low, with typical surface enhancement factor ranging from 10 to 10^3 depending on the metal and surface preparations.[43,44]

It should be noted that in using the electrochemical roughening method in general it is difficult to obtain a uniform surface at both macro- and microscopic level. There is a broad distribution of surface structures with grain sizes ranging from nanometers to microns. Thus, only a portion of surface structures plays a major role in the observed SERS activity. Considering that the SERS activity is strongly shape dependent,[59,60] we and Xia's group have synthesized and studied TM nanoparticles with some special shapes, such as Pt and Pd nanocubes for SERS study.[61–63] It has been shown that the SERS activity from these well-ordered and good-shaped nanoparticles is higher by a factor of 3–10 than the roughened electrodes.[61] However, there still remains a considerably large gap between the TMs and typical SERS-active substrates as far as the SERS activity is concerned. As a consequence, SERS signals are rather weak or even below the detection limit from some adsorbates with a very small Raman cross section or with a low surface coverage. Therefore, it is desirable to increase the SERS activity in order to improve molecular generality of SERS for transition metals of practical and fundamental importance.

Development of strategy of borrowing SERS activity

Aiming to expand the generality of Raman spectroscopy by fully optimizing the SERS activity of the TM based systems, we have recently incorporated a strategy of "borrowing" high SERS activity from the Au core. The approach of "borrowing SERS activity" was initially proposed by Van Duyne *et al.* in 1983 to obtain Raman signals of molecular species adsorbed on non-SERS-active materials such as n-GaAs electrodes through electrodepositing a discontinuous SERS-active overlayer of Ag.[64–66] This approach is to employ the long-range effect of the very strong electromagnetic field created by the SERS-active Ag to enhance the Raman scattering of adsorbates at the semiconductor nearby. As illustrated in Fig. 1(a), this configuration has a limitation for studying surface adsorption, which requires that the surface species can selectively be adsorbed at the non-SERS-active substrate. In fact, most molecules studied prefer to adsorb at the SERS-active islands.

The most effective and feasible way to borrow SERS activity is to coat with an ultrathin film of other materials completely on SERS-active substrates of Ag as done by the Fleischmann group[67,68] and Au by the Weaver group,[69–71] respectively, in 1987 and later. The essential notion rests on the expectation from electromagnetic (EM) theories that the enhancement effect should occur, albeit in attenuated form, for molecules located close to (within 1–10 nm) SERS-active nanoparticles or nanostructured surfaces.[53,72–74] With the aid of the long-range effect of the enormous electromagnetic enhancement created by the high SERS-active substrate underneath, the Raman enhancement can be engendered even for molecules spatially separated from the SERS-active substrate (see Fig. 1(b)). As a consequence, good-quality SERS spectra of adsorbates on several TM film electrodes have been obtained.[67–72] It should be noted that the strong electromagnetic field will be attenuated exponentially with increasing thickness of the "spacer" film, therefore the film has to be ultra-thin, normally a few atomic layers. However, it was very difficult to cover completely the very irregular roughened surfaces with so thin a film, as illustrated in Fig. 1(b). Although pinhole-free ultrathin films of some TM overlayer electrodes have been successfully achieved by carefully optimizing the electrochemical deposition parameters in the

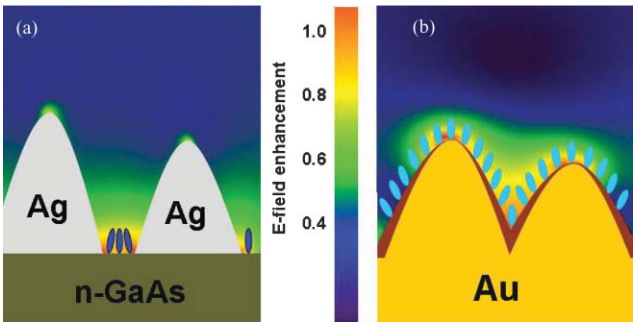

Fig. 1 Schematic illustrations of the two strategies of borrowing SERS activity. (a) Deposit discontinuous SERS-active metal islands on the substrate to study the molecules adsorbed on the substrate; (b) Coat an ultrathin non- or weak-SERS-active layer on the SERS-active substrate to study the molecules adsorbed on the layers.

late 1990s,[75–78] this very delicate method has some inherent difficulties to be widely used for different materials and has not been adopted by other groups.

In 2002, a great step forward along this direction was made by Weaver and co-workers by fabricating Pt-group metal-coated Au nanoparticles dispersed electrodes.[79] They first immobilized the gold particles onto a functionalized indium tin oxide (ITO) electrode *via* the interaction with amine groups. An underpotential deposited (UPD) monolayer of copper was then formed on the nanoparticles film by warily controlling the applied potential. Finally the electrode was transferred to a solution of 5 mM $PdCl_2$ or H_2PtCl_4 to allow spontaneous redox replacement of the Cu layer by the Pt-group metal. The virtue of this combined UPD and chemical redox replacement method is that it provides a uniform (pinhole-free) growth of one atomic Pt layer on the spherical Au nanoparticles. The SERS signal is remarkably more intense than the TM coated Au electrodes[79] because the Au nanospheres with well-defined shape and size exhibit very high SERS activity that can be sufficiently borrowed through the ultrathin Pt shell, as illustrated by Fig. 2. However, the whole preparation procedure of this method, involving the surface functionalization, electrochemical UPD and chemical reaction, is quite complicated. To obtain thicker overlayers, multiple growing cycles involving electrochemical and chemical reactions are needed to take place in sequence by repeatedly changing the solution. It is therefore highly desirable to develop a simpler and straightforward method to prepare TM-coated Au nanoparticles for improving the substrate generality.

Regarding the lack of surface generality, it is crucially important to seek other borrowing ways to create the SERS activity on atomically flat single crystal surfaces. One way is to excite the surface plasmon polaritons (SPP) on the flat metal surface by using a unique optical configuration setup. By illuminating p-polarized light at a suitable angle through a Weierstrass prism on a gap half of the exciting wavelength formed by the prism and a single crystal surface metal surface, the SPP can be excited within the gap, which will lead to an enhancement of the electromagnetic field and improved sensitivity of Raman spectroscopy. A SERS study using an attenuated-total-reflection (ATR) Raman cell with the Otto configuration on truly smooth single crystal surfaces under electrochemical conditions was reported by Otto and co-workers recently.[80] The enhancement, assisted by the surface plasmon enhancement, for a single-crystal Cu surface is estimated to be around one to two orders of magnitude. Another type of ATR Raman cell with the Kretchmann configuration has also been used to obtain SERS from an Ag(111) surface, as well as from Pt and Ni surfaces.[81] However, this optical configuration requires depositing the metal as an ultrathin film on the quartz substrate, which is not feasible to prepare various metal surfaces as well-defined single crystal surfaces. Overall, there are only a very limited number of molecules with very weak SERS signal that have been detected by these two delicate ATR setups. As mentioned above, the surface plasmon enhancement can be efficiently excited only on Au, Ag and Cu metals. This optical setup of borrowing SERS activity seems not to be widely adoptable to study single-crystal surfaces of other non-traditional SERS-active materials including the TMs.

Recently, there has been a great progress along the direction of the borrowing strategy to solve the problem of the surface generality of SERS by employing tip-enhanced Raman spectroscopy (TERS).[82–88] The idea of tip-enhanced Raman spectroscopy was first put forward by Wessel in 1985,[82] and realized in 2000 independently by several groups[83–86] and has brought about a surge in these two years demonstrating both very high spatial resolution and high sensitivity.[87,88] In TERS, the enhancement generated on the tip under the excitation of a suitable laser can extend to the sample that is in close proximity to the tip apex, as illustrated in Fig. 3. Therefore, the sample borrows the enhancement from the tip itself or, if possible, the coupled enhancement from the tip and sample. With this borrowing enhancement strategy, the surface Raman signals (or TERS signal) from adsorbed species have been obtained from smooth or roughened surfaces with different structures and of different materials, which has expanded greatly the surface and substrate generalities.

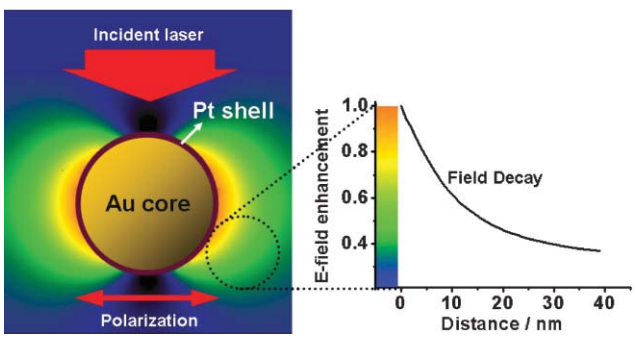

Fig. 2 Schematic illustration of the electromagnetic field distribution around Au@Pt core–shell nanoparticles under laser irradiation (left). The dependence of the electromagnetic field strength (normalized with the strength on the Pt surface) on the distance from the Pt shell is shown in the right plot, indicating a substantially strong field enhancement can still be obtained on the surface.

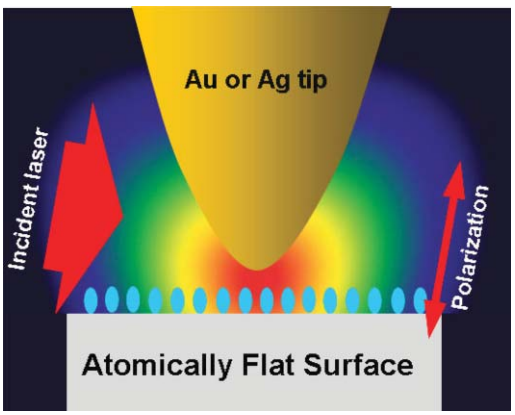

Fig. 3 A schematic illustration of the working principle of tip-enhanced Raman spectroscopy: light with appropriate wavelength and polarization is illuminated at the gap between the tip and the surface, producing an enhanced electromagnetic field at the nanogap and hence an enhanced Raman signal for the species adsorbed at the substrate.

To fully accomplish the borrowing SERS activity strategy and optimize the nanostructures, it is important to predict the shell thickness and/or effective distance from the highly SERS-active core or tip through performing theoretical models and calculations. It is well known that the main contribution to the SERS and TERS effect is in general the electromagnetic (EM) field enhancement that originates from localized surface plasmon resonance of nanostructures. The EM field of the incident light at the surface can be greatly enhanced under conditions of localized surface plasmon resonance for 'free-electron' metals.[18,35,52–56] Most of previous theoretical studies on the EM enhancement were limited on metal nanosphere systems[25,89,90] since the analytical solution for the Maxwell equations can only be obtained on such systems with high symmetry through Mie scattering theory. For more complex geometries, one has to rely on numerical simulations to quantitatively solve the problem of electromagnetic effects. Finite difference time domain (FDTD) method,[61,91–94] discrete dipole approximation (DDA),[95–97] finite element method (FEM)[98–100] and T-matrix method[101] are widely used to numerically solve the near field distribution problem for any arbitrary geometry. Among them, FDTD is a powerful tool to simulate the electromagnetic field distribution around illuminated nanoparticles or substrate with any arbitrary geometry.[102] In order to simulate the SERS or TERS systems with FDTD, one has to deal with the dispersive materials since the complex permittivity of all of the metals in the optical frequency range are strongly frequency dependent. This model has shown great consistency with Mie theory in a previous study to deal with the electric field enhancement problem in a multiple silver nanosphere system.[103]

This article aims to present our contributions in extending substrate, surface and molecule generalities in recent years utilizing the borrowing strategy to increase the SERS activity of TMs and to obtain the SERS signal from atomic flat surfaces. The article is organized in following three sections. In the first section, we will introduce the fabrication of SERS-active Au@TM nanoparticles film electrodes that were used as SERS substrates to boost the detection sensitivity for the processes occurring on TM SERS systems. The total enhancement of as high as about four to five orders of magnitudes has been achieved, which makes it possible to carry out detailed molecular-level investigation on some important molecules with small Raman cross section. With such a high enhancement, we have been able to obtain the SERS signal of water molecules adsorbed on TMs, which were impractical and extremely difficult by using the enhancement of SERS of TM themselves. In the second section, we will introduce a new emerging technique, tip-enhanced Raman spectroscopy, for studying processes occurring on single-crystal Au and Pt surfaces, by borrowing the enhancement from the tip. To explain the experimental observations, a three-dimensional finite-difference time-domain (3D-FDTD) method was used to calculate and evaluate the local electric field on TM coated nanoparticle surfaces and the TERS tips. In the final section, prospects and further developments in SERS techniques based on the borrowing strategy are briefly discussed.

Expanding substrate generality of SERS by core–shell nanoparticles

Preparation of Au@TM nanoparticles film electrodes

Bearing in mind the advantages and disadvantages of the above mentioned approaches, we have recently developed a simpler and more straightforward method to prepare TM-coated Au nanoparticles based on a seed-mediated growth method.[61,104,105] Au nanoparticles serve as the seed in a solution where a second metal ion is chemically reduced on the surface of the seeds to form a shell layer, resulting in core–shell nanoparticles. Fig. 4 illustrates the procedure for preparing Au@TM nanoparticles film electrodes (here we take Au@Pd as example). First, highly mono-dispersed Au nanoparticles are synthesized according to Frens' method by reducing $AuCl_4^-$ with sodium citrate[106] and a 1.0 mM H_2PdCl_4 aqueous solution was prepared by dissolving 88.6 mg $PdCl_2$ in 11 ml of 0.1 M HCl under heating and stirring. After cooling to room temperature, the solution was diluted to 500 ml. Secondly, the Au core was coated with one to ten atomic layers of the desired TM according to the method reported in refs. 107 and 108 with slight modification: in a typical procedure to prepare Au@Pd nanoparticles, 30 mL sol containing Au seeds was first mixed with a certain amount of 1 mM H_2PdCl_4 and the mixtures were cooled to *ca.* 4 °C in an ice-bath; then, half the volume of 10 mM ascorbic acid to that of H_2PdCl_4 was slowly dropped into the above mixture through a syringe controlled by a step motor while stirring; afterwards, the mixture was then stirred for another 15 min to ensure a complete reduction of H_2PdCl_4, during which the color of the mixture turned from red–brown to dark-brown, indicating formation of Au@Pd nanoparticles.[109] Thirdly, the Au@Pd nanoparticles sol was centrifuged three times to remove excess reactants and to obtain a clean surface. Finally, about 25 μL aliquot of the remaining sol was cast on a mechanical polished and electrochemically cleaned electrode, which was then dried in a desiccator for about 20 min. Such an electrode is ready for SERS measurement. Other Au@TM/electrodes (TM: Pt, Rh, Ru, Co or Ni) can also be prepared using a similar chemical method with different solutions and at different temperatures.[110]

The virtue of the present method for preparing core–shell nanoparticles is that the shell thickness from one to ten atomic

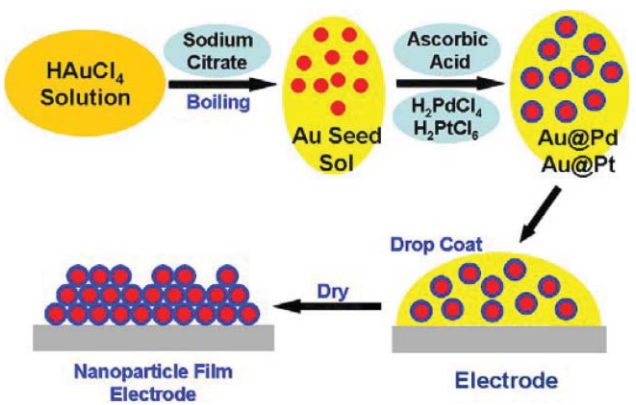

Fig. 4 Schematic representation of the four steps for preparing the Au@Pt and Au@Pd nanoparticles film electrodes.

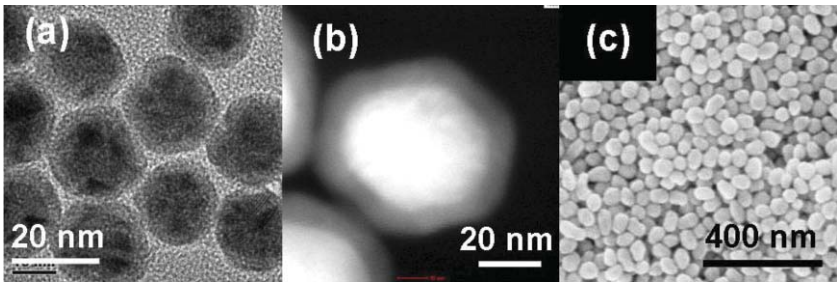

Fig. 5 Typical TEM (a) and STEM (b) images of Au@Pd nanoparticles and an SEM (c) image of a Au@Pd nanoparticle-assembled film electrode surface.

layers can be routinely controlled by adjusting the ratio of the amount of the Au seeds to the TM ions. For example, the thickness of the Pd shell is controlled by changing the volume of H_2PdCl_4 solution added while keeping the volume of Au seeds constant. The final diameter (D) of the core–shell nanoparticles can be calculated according to the relation:[105,107]

$$D = D_{\text{core}}\left(1 + \frac{V_{\text{m,Pd}}N_{\text{Pd}}}{V_{\text{m,Au}}N_{\text{Au}}}\right)^{1/3}$$

where D_{core} is the diameter of the experimentally measured Au seeds, $V_{\text{m,Pd}}$ and $V_{\text{m,Au}}$, and N_{Pd}, and N_{Au} are the molar volumes and molar number of Pd and Au, respectively. Therefore, the shell thickness can be estimated by $(D - D_{\text{core}})/2$.

Fig. 5 shows the transmission electron microscope (TEM) and scanning transmission electron microscope (STEM) images of the nanoparticles with a Pd shell of about 7 nm thick. The TEM and STEM images were collected on Tecnai F30. From the TEM image, a dark core surrounded by a light-color shell can be clearly distinguished, indicating a core–shell structure of the nanoparticles. When we used Pd to collect the STEM images, we obtained images with very clear ring structure, indicating a core–shell structure. The energy dispersive X-ray spectroscopic (EDS) measurements of single nanoparticles revealed that the edge consists of nearly pure Pd, while the center consists of both Au and Pd, further demonstrating the core–shell structure. Fig. 5(c) shows the SEM image of a 55 nm Au core covered with 1.4 nm Pd shell dispersed as a complete thin film on a Pd electrode (hereafter denoted as 55 nm Au@1.4 nm Pd/Pd). The surface of the film electrode is very uniform containing nanoparticles with a very narrow size distribution. The surface shows a golden color under daylight visible to the naked eye. Concerning the stability of the nanoparticles film electrodes, it has been found that the core–shell nanoparticles can form a multilayer thin film and attach tightly on the electrode surface.[105]

The most important but difficult part of this strategy is how to well-controllably fabricate core–shell nanoparticles showing very large surface enhancement on the TM surface but having the chemical properties of the TMs. Since the strong EM field is attenuated substantially from the Au core surface to outside space, as shown in Fig. 2, the thinner the shell is the higher the borrowed SERS activity will be. However, one must be very cautious to avoid pinhole effects when the shell thickness is less than three atomic layers. The ultrathin shell may not be sufficient to completely cover the Au core and some tiny areas of the Au core may be exposed. The comparably strong SERS signal of molecules on the pinholes may mix with the SERS signal from the shell which may then mislead the interpretation of the SERS spectrum. Therefore, to well apply the borrowing SERS strategy to a wide range of materials, the shells must be suitably uniform and, ideally, free of pinholes.

It should be pointed out that HRTEM and STEM are not appropriate tools to check whether there are pinholes in the shell as thin as a few atomic layers. Alternatively, we adopted electrochemical and SERS methods used by Zou and Weaver to identify the tiny pinholes in the shell.[75] Cyclic voltammetry, as a surface sensitive technique, can be used to examine the coating quality of the nanoparticles, *i.e.*, to check whether there are pinholes on the shell.[75] Fig. 6 shows cyclic voltammograms of a 55 nm Au@1.4 nm Pd/GC electrode and a 55 nm

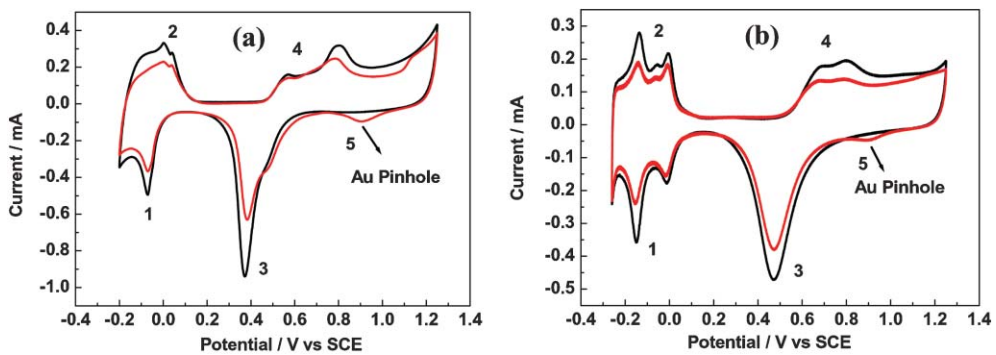

Fig. 6 Cyclic voltammograms of a 55 nm Au@1.4 nm Pd/GC electrode (A) and a 55 nm Au@1.4 nm Pt/GC electrode (B) without (black line) and with "pinholes" (red line) in 0.5 M H_2SO_4 solution. Scan rate: 100 mV s^{-1}. The peaks marked in the figures correspond to: (1) hydrogen adsorption; (2) hydrogen desorption; (3) reduction of Pt or Pd oxides; (4) oxidation Pt or Pd; (5) reduction of Au oxides.

Au@1.4 nm Pt/GC electrode in 0.5 M H_2SO_4 at a scan rate of 100 mV s^{-1} in the potential regions between −0.20 and 1.25 V and between −0.26 and 1.25 V, respectively. Both figures show the typical feature of pure polycrystalline Pd and Pt electrodes, with characteristic peaks of hydrogen adsorption/desorption, oxygen adsorption/desorption as well as Pd and Pt oxidation/reduction, indicating that the surface chemical property is identical to that of a typical bare Pd and Pt electrode. Only when the electrode potential was kept at 1.25 V (the oxidation potential of both metals) for a few minutes for Pd and a few hours for Pt, did the voltammograms show a small reduction peak at around 0.9 V as characteristic of an Au electrode, indicating that the original pinhole free Pd and Pt shell has been damaged and a small amount of Au sites have been exposed.

A more straightforward way to examine the pinhole is to perform a SERS measurement using CO as the probe molecule for the following three reasons: (i) CO can be adsorbed at TMs as a monolayer and exhibits a relatively strong SERS signal. (ii) The CO stretch band is rather sharp and its frequency is very sensitive to the properties of the substrate. For example, it will give a different frequency and spectral feature when it is adsorbed at the pure TM, the alloy surface formed by TM and Au, and the exposed Au sites as the pinhole. (iii) Even for the same substrate, CO can sensitively reflect the small differences in the electronic property or structure when the shell thickness changes. The stretch frequency of CO adsorbed on Au (at *ca.* 2120 cm^{-1}) is distinctively different from that on the TM surfaces (below 2100 cm^{-1}). If this band can be detected, the shell must contain pinholes. However, if it can not be detected, the effect of pinholes can be neglected or the shell is pinhole free.[75,110]

It should be noted that a surface with good uniformity is crucially important to the reproducibility of our experiment. To check the uniformity, Raman mapping experiments were performed by scanning the laser over different regions of the whole surface of Au@Pt/electrode with a scanned area of 50 μm × 50 μm. We found that the maximal difference in the SERS intensity over all the scanned areas is only about 10%.[105] Au@Pt/electrodes show not only very good surface uniformity, but also much higher SERS activity, which is a prerequisite of SERS for the reliable study, especially quantitative analysis.[111]

SERS activity of Au@TM nanoparticles film electrodes

To examine the SERS activity of Au@TM/electrodes, here we take the Pt system as example. The comparative experiment was carried out using CO as the probe molecule on three types of SERS substrates, *i.e.*, electrochemically roughened Pt electrode, 12 nm nanocubes/glassy carbon electrode and 55 nm Au@1.4 nm Pt/Pt electrode. As can be seen from Fig. 7, the SERS signal from the core–shell nanoparticles film electrode is about 40-fold stronger in peak intensity and integrated intensity, respectively, than the nanocubes film electrode, and about 200- or 80-fold stronger than the roughened Pt electrode. It should be noted that the intensity scale of Fig. 7(b) and (c) have already been multiplied by 20 and 100, respectively. Taking account of the roughness factor of the roughened Pt

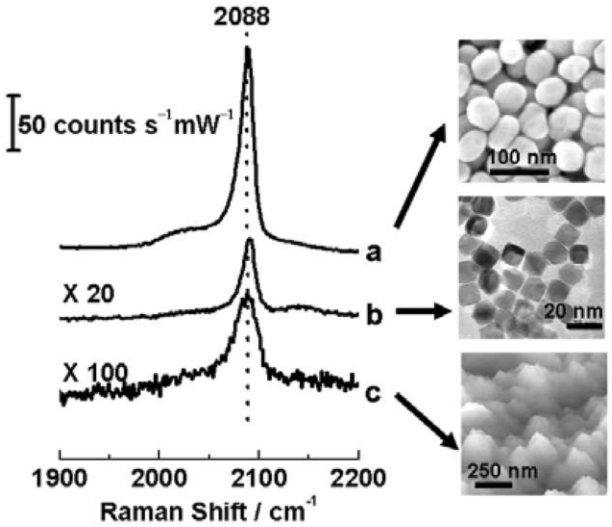

Fig. 7 SER spectra of adsorbed CO on different substrates: (a) 55 nm Au@1.4 nm Pt/Pt; (b) 12 nm Pt nanocubes/Pt; (c) roughened Pt electrode. The solution is CO-saturated 0.1 M $HClO_4$ and the potential was 0.0 V.

electrode to be about 120, and that for the two nanoparticles film electrodes is about 10, one would expect the surface enhancement for the core–shell nanoparticles to be about 27-fold larger than that of nanocubes and 640-fold larger than that for the roughened Pt electrode.

Besides the significant difference in intensity, we also note that the difference in the band width. For instance, the band width for CO stretching on the roughened Pt is *ca.* 27 cm^{-1}, whereas it is *ca.* 15 cm^{-1} on the nanoparticles surfaces. The main reason is due to the ill-defined structure of the roughened electrode because the CO band frequency is very sensitive to its adsorbed site and environment. This result further demonstrates that the well controllably synthesized nanoparticles and nanocrystals have a more uniform surface in comparison with the electrochemically roughened electrodes.

Besides Au@Pd and Au@Pt nanoparticles, we have also synthesized Au@Ni, Au@Co and Au@Rh nanoparticles to broaden the application of core–shell nanoparticles.[112a] To compare their signal intensities with that from roughened massive electrodes, we took pyridine as the probe molecule. It can be seen in Fig. 8 that the SERS signals from core–shell nanoparticles film electrodes are stronger than massive metal electrodes, which is about 40-, 35- and 50-fold for Pt, Pd, and Ni, respectively. Considering the roughness factor of the core–shell nanoparticles film electrodes is about 15, we can estimate the surface enhancement factors for these 55 nm Au@1.4 nm TM nanoparticles to be about 1.0×10^4, 5.3×10^3, and 1.0×10^4 for Pt, Pd, and Ni, respectively. They are about one order or more of magnitude larger than that obtained on massive metal electrodes.

To quantitatively account for the SERS activity of the core–shell nanoparticles system, we use the 3D-FDTD method to calculate electromagnetic field distribution around the illuminated nanoparticles (refer to ref. 61 for detailed description of the calculation method and parameters). A model consisting of two Au@Pt nanoparticles was used to take

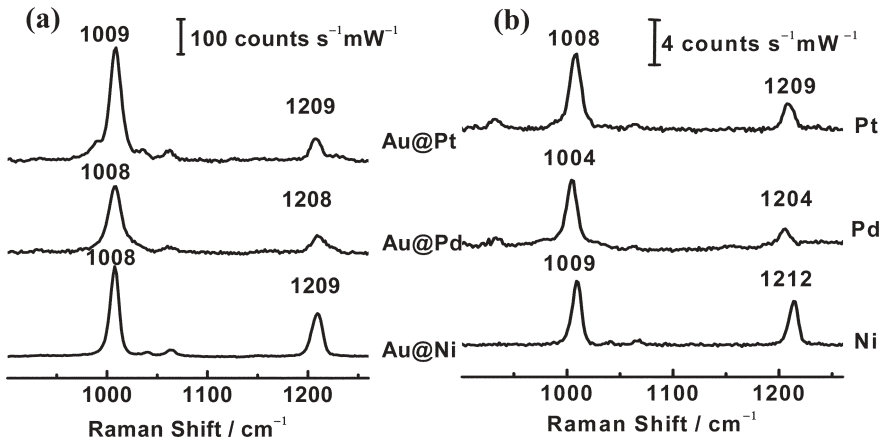

Fig. 8 SER spectra of pyridine adsorbed on (a) 55 nm Au@TM/GC with different TM (Pt, Pd and Ni) shells with a thickness of 1.4 nm and (b) roughened massive TM electrodes in 0.01 M pyridine and 0.1 M $NaClO_4$ solution. The potential is −0.6 V for Pt and Pd, and −0.9 V for Ni.

account of the EM field coupling effect as the core–shell nanoparticles are aggregated on the electrode surface in the experiment. Fig. 9 shows the simulated electric-field distribution of the Au@Pt–nanoparticle dimer. The shell thickness is set to be 1.5 nm, the core size 55 nm, and the interparticle distance 1 nm. The 632.8 nm excitation laser is polarized along the axis connecting the two particles and the laser is irradiated perpendicularly to the surface plane. The Yee cell size used in the calculation was 0.5 nm × 0.5 nm × 0.5 nm, and the total number of time steps was 15 000 to ensure the convergence. The calculated data show that at the junction of two nanoparticles, the maximal field enhancement is about 112, corresponding to 1.6×10^8 of the Raman signal enhancement. This value is much higher than that of two pure 55 nm Pt nanospheres.[112b] In the latter case, the maximum EM-field enhancement is about 45, corresponding to *ca.* 4×10^6 of the enhancement factor. By comparing the two enhancement factors, one may deduce that about two orders of the SERS enhancement may borrow from the long-range EM effect of the gold core.

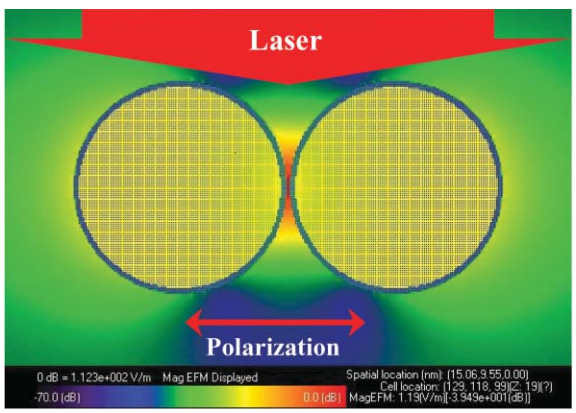

Fig. 9 A simulated representation of the electric field distribution around a Au@Pt nanoparticle dimer (core size 55 nm and shell thickness 1.5 nm). The 632.8 nm laser is illuminated with the polarization along the connecting axis of the two particles.

It has been pointed out that when two nanoparticles approach each other, the electromagnetic theory predicts that a coherent interference of the enhanced field around each particle will result in a dramatic increase in the electric field in the junction between them.[113] Accordingly, the calculated electromagnetic field is highly localized at the junction of two particles, as shown in Fig. 9. It can be seen clearly that the magnitude of the electric field reaches the maximum in the gap region of the dimer. Since the SERS signal obtained in the experiment should average over all the surfaces, therefore, the enhancement obtained in the experiment may be substantially lower than the calculated value. Nevertheless, the ratio of enhancement factors for the bimetallic core–shell and monometallic sphere systems may still reflect the real difference in enhancement between these two systems.

It may also be necessary to emphasize that any rigid calculation should take into account the size-dependent dielectric function, as has been reported on the simulation of Ag nanoparticle systems.[56,114–116] In fact, for core–shell nanoparticles, the electron–surface collision could dominate the damping mechanism of the plasmon response of the Pt shell rather than electron–electron collisions in the bulk metal. However, in the present simulation of Au@Pt, the dielectric constants of the ultra-thin shell were directly taken from the value of the bulk metal rather than a size-dependent dielectric constant, because we still lack the necessary parameters, including Fermi velocity and bulk plasmon frequency of Pt, in order to make an appropriate modification. Fortunately, the decay originating from the size-dependent dielectric constant for Pt is not as dramatic as for Ag in the visible light region. One of the reasons may be the electron mean free path of TMs is much smaller than that of Ag, *e.g.*, 12 nm for Pt, *cf.* 43 nm for Ag.[117,118] Therefore, the imaginary component of dielectric constant for TMs will result in a relatively small damping effect compared with Ag. As a result, the modification on the dielectric function will have less influence on Pt systems than Ag. However, in future work, it is still necessary to pay more attention to the changes of the size-dependent dielectric constant especially when the thickness of the TM shell is less than 2 nm.

Dependence of the SERS activity on the shell thickness and core size

Both the experimental and theoretical results confirm that the high SERS activity achieved in ultra-thin shell systems is attributed to the long-range effect of the enhanced electromagnetic field generated by the Au core. Since SERS is an effect sensitive to the size and detailed structure of the nanoparticles, it is necessary to find out the optimized shell thickness and Au core size for expanding the substrate generality most effectively. Accordingly, we performed a systematic study on the dependence of SERS intensity on both the shell thickness and core size.

In the thickness dependent experiment, we used Au cores with a diameter of 55 nm because they can be most easily prepared with the best reproducibility and narrowest size distribution (*vide infra*). Up to now, Pt, Pd, Rh, Ni and Co have been successfully coated over Au core to form core–shell nanoparticles with controllable shell thickness. In the case of Pd, the thickness of the Pd shell could be controllably changed from 0.7 to 6.8 nm, equal to about 2.5 to 24 atomic layers of Pd.

Fig. 10(a) presents a set of SERS spectra of CO adsorbed at an Au@Pd/GC electrode. The bands at about 1951 and 2062 cm^{-1} are assigned to bridged and linearly-bonded CO, respectively. As expected, the SERS intensity of CO decreases significantly with increasing shell thickness. In other words, the thinner the Pd shell, the higher the SERS activity of the Pd substrate. To more quantitatively investigate the effect of the shell thickness on the SERS intensity, we plotted the integrated intensity (normalized with the signal obtained at 0.35 nm thickness) of the CO stretching band against the thickness, and the result is presented in Fig. 10(b) as the open circle together with the error bar. It can be seen that the signal decreases exponentially with increasing thickness and a 2.5 monolayer Pd shell gives about 8-fold higher intensity than that of the 24-monolayer case. For comparison, we carried out a FDTD simulation of such a system. Due to the unrealistic calculation demand on considering the thickness of 0.35-nm, the thinnest shell thickness is set to 0.5 nm, and the theoretical data shown in Fig. 10(b) have been normalized with 0.5 nm intensity. It shows essentially the same trend as the experimental result.

As far as the SERS signal intensity is concerned, it seems a thinner shell thickness is better for producing highest signal intensity based on the above experimental and theoretical results. However, in the application of such core–shell nanoparticles, one must consider another important factor in addition to the pinhole problem, *i.e.*, whether the ultrathin shell is well representative of the massive metal in terms of the electronic property. When Au and Pd are in good contact, electron transfer will occur due to the difference in the Fermi level of two metals. As a consequence, the electronic property of the ultrathin shell will be changed by the core to some extent.

Carefully examining the frequencies of CO adsorbed at the Au@Pd/GC electrode shown in Fig. 10(a), one can see that the frequency is at *ca.* 1951 cm^{-1} when the thickness is less than 1.4 nm (about five atomic layers of Pd). However, the frequency shifts to 1958 cm^{-1} when the shell is about 1.4 nm or thicker. This mild difference in frequency could be due to the difference in the electronic property of the ultrathin metal film. There have been several studies on the electrochemical reactivity of ultrathin TM layers epitaxially deposited on massive Au substrates.[75,78,119,120] For instance, Kolb and co-workers found that the potential of zero charge Pd coated on Au(111) is practically identical to that of massive Pd(111) when there are five monolayers of Pd in their study on the thickness dependent electrochemical reactivity of electrodeposited palladium thin layers on Au(111) surfaces.[119] It seems that the electronic property of a five atomic layer thick film could be reasonably similar to that of the massive metal.

As Au@TM nanoparticles are coated over an electrode substrate to form the film electrode, the electronic property of the TM shell could also be influenced by the well-contacted substrate. We intentionally coated the core–shell nanoparticles on a substrate of the same metal as the shell, *i.e.*, as Au@TM/TM electrode. As a consequence, the electron property of the shell could be close to that of the bulk TM substrate, which could eliminate the influence by the electron transfer between the Au core and TM shell. Accordingly, we have in general used Au@TM/TM electrodes for electrochemical potential-dependent SERS measurements.

Concerning the shell dependence of optical property of the core–shell nanoparticles, UV-vis absorption spectroscopy is

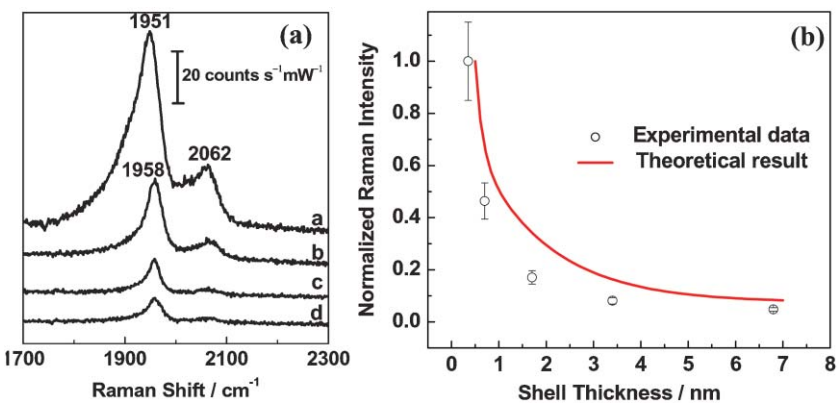

Fig. 10 (a) SER spectra of CO adsorbed on 55 nm Au@Pd/GC with different Pd shell thicknesses in CO-saturated 0.1 M $HClO_4$ at 0.0 V: (a) 0.7 nm; (b) 1.4 nm; (c) 2.8 nm; (d) 6.8 nm. (b) Dependence of the intensity of CO adsorbed on 55 nm Au@Pd on the thickness of Pd shell (open circles) and the corresponding FDTD calculation result (red line).

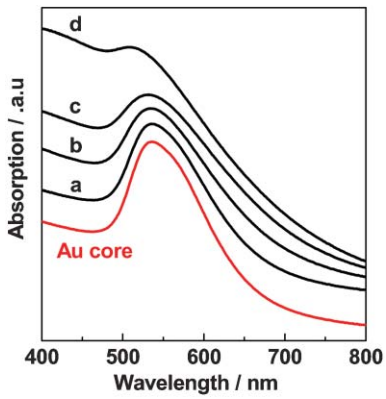

Fig. 11 UV-visible absorption spectra of 55 nm Au (red line) and Au@Pd nanoparticles (black lines) with different thicknesses of the Pd shell: (a) 0.35 nm, (b) 1.4 nm, (c) 2.8 nm and (d) 6.8 nm. The curves were displaced along the *y*-axis for clarity.

the most suitable technique. Fig. 11 presents a series of UV-vis spectra obtained in the sols of Au@Pd nanoparticles with fixed core size of 55 nm and varying shell thickness. The spectrum of the corresponding Au core is also given for reference, which has been offset for clarity. It can be seen that as the Pd shell becomes thicker, the plasmon absorption of Au core slightly blue shifts and is gradually damped. Meanwhile, the absorption in the low wavelength region increases steadily. These spectral behaviors reasonably infer that the total optical properties of the core–shell structure changes from core dominant to shell dominant as the shell thickness increases. Unlike a sharp absorption band for Au spherical nanoparticles, pure Pd nanoparticles show a rather broad and strong absorption in the 200–800 nm region.[121a] Thus, when the Pd shell becomes as thick as 6.8 nm, the plasmon of Au core can be completely damped showing the similar absorption feature to that of pure Pd nanoparticles. While Au@Pd nanoparticles with 1.4 nm Pd shell thickness show almost identical spectral feature to that of bare Au nanoparticles and identical chemical properties to that of the bulk Pd. After carefully trading off among the SERS enhancement, pinhole effect, shell stability and electronic property, we prefer to use the shell thickness of about five layers as the optimal condition in most of the electrochemical SERS studies.

To investigate effect of core size, we synthesized Au cores with diameters from about 15 nm up to 160 nm, which were then coated with a fixed shell thickness of 0.7 nm (about two atomic layers of Pd) to fully utilize the SERS activity of the core. It can be seen from Fig. 12 that, the SERS intensity of the adsorbed pyridine increases considerably with the increasing size of the Au core until 135 nm, which is in good agreement with the theoretical prediction.[121b] This result indicates that it is better to use gold cores with larger size to obtain the highest enhancement. However, we have found that with the increase in the size of the Au nanoparticles, the shape and size distribution of the nanoparticles becomes broader, and the nanoparticles can easily form aggregates and even precipitate from the sol solution with time. Therefore, we used the 55 nm core as the optimal condition in the present study. If the problem associated with the large nanoparticles can be

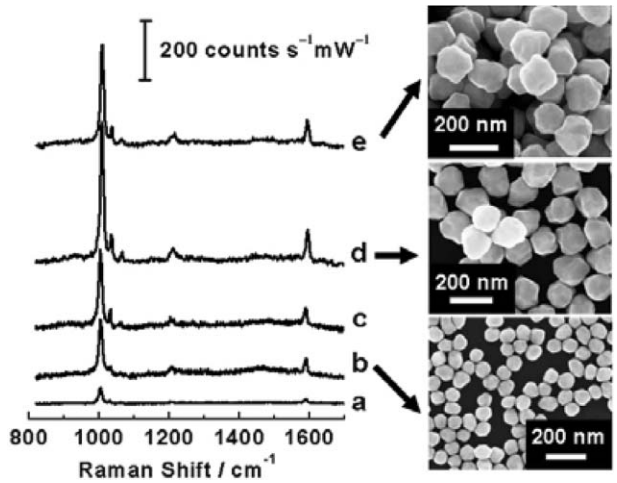

Fig. 12 SER spectra of pyridine adsorbed on Au@0.7 nm Pd/GC with different Au core sizes in 0.01 M pyridine and 0.1 M $NaClO_4$ solution: (a) 40 nm, (b) 80 nm, (c) 120 nm, (d) 135 nm, (e) 160 nm. Shown on the right side are the typical SEM images of nanoparticles with a diameter of 80 nm, 135 nm and 160 nm.

solved in the near future, we believe that Au cores with a diameter of about 110–130 nm can be used as the optimal core size.

After thoroughly considering all factors influencing the structure and properties of Au@TM/electrodes, we have synthesized Au@TM/electrodes with suitable shell thickness and free of pinholes, and demonstrated that the optimized nanostructures can exhibit very high surface enhancement and provide unprecedented detection sensitivity of SERS from TMs. This technique based on the borrowing SERS activity strategy is especially valuable for expanding the substrate generality of Raman spectroscopy. It opens up a way to study some important molecules, such as surface water molecules, adsorbed at TMs, which is very difficult or even impractical to study by Raman spectroscopy including SERS.

Expanding the molecule generality to surface water on transition metals

It is well known that water plays vital roles in many chemical processes. The water molecules in regions immediately adjacent to metal surfaces can directly affect electrochemical processes and reactions. Raman spectroscopy has the capacity to probe electrode/aqueous solution interfaces by directly illuminating the interface with a visible laser beam and collecting the scattered light through the aqueous solution phase because the Raman cross section of water is very small. Unfortunately this significant advantage turns to be the major disadvantage when the surface species to be characterized is the water molecule itself. As a consequence, conventional Raman spectroscopy is impractical to probe surface water molecules at metal electrodes, unless the highly SERS-active substrates of Ag, Au and Cu are used.[122–125] Since the late 1990s when good-quality SER spectra from various TMs were obtained, we have intensely challenged, but unfortunately failed, to obtain SERS of water from any of the weak-SERS-active TMs.

Considering the low enhancement factor of bare TMs at only around 10^2 to 10^3, it is worth utilizing the borrowing strategy with the core–shell nanostructures, from which SERS signals can be enhanced by about two orders of magnitude in comparison to those from bare TM nanoparticles or electrodes.[61] This additional enhancement may allow us to detect SERS signal from water molecules with a small Raman cross section that has been hitherto impractical to study on TMs.

For a systematic study, two types of core–shell nanoparticles were synthesized with 55 nm Au cores covered with 1.4 nm Pt and Pd shells, then coated as a thin film on smooth Pt or Pd electrode surfaces, respectively. Fig. 13 shows SERS spectra of water adsorbed on Pt and Pd surfaces in comparison with the typical SER spectrum of water adsorbed at a highly SERS-active Au electrode in 0.1 M $NaClO_4$. Two bands located at around 1615 and 3400 cm^{-1} are assigned as the bending and stretching vibrations of water molecules. To confirm that the surface species showing the SERS signal are from water instead of solution impurities, we also performed an isotopic measurement to replace the normal water with heavy water. All the spectral bands are shifted according to the isotopic effect, as shown in Fig. 13(d). The spectra of water show the characteristics of strong potential dependence in frequency and/or intensity, convincingly demonstrating that these signals must be derived from the surface water molecules rather than from bulk water.[126]

In spite of the fact that the SERS signals from the TM substrates are rather weak, especially for the bending vibration, these are the first Raman spectra of surface water from TMs. Without the about two orders of amplification borrowed from the Au core, the Raman signal from surface water would be overwhelmed in the noise level because of the weak SERS activity of bare TMs. On the other hand, the SERS intensities on Pt, Pd and Rh are only about 30- to 50-fold lower in magnitude than that of Au, indicating that the high electromagnetic enhancement of the Au core has effectively boosted the Raman signal of interfacial water molecules on shell metal surfaces.[126]

It is of special interest that a broad and weak band at around 2000 cm^{-1} is observable only on the Pt surface, see Fig. 13(a). This is ascribable to the Pt–H stretching vibration mode in the potential region negative of −1.0 V (*vs.* SCE).[51c] Hydrogen is strongly adsorbed on the Pt surface whereas it is absorbed in bulk Pd and interacts with Au much more weakly. To our knowledge, this is the first Raman (also SERS) spectra of surface hydrogen co-existing with surface water.

It has been found that the extent of the frequency shift with potential (*i.e.*, vibrational Stark effects) for the stretching mode of water on Pt is significantly less than those of the Pd and Au electrodes. The Stark tuning rate is only about 14 cm^{-1} V^{-1} for Pt but about 64 and 76 cm^{-1} V^{-1} for Au and Pd, respectively. This indicates that the structure of interfacial water should be different for these three metals.[126] In order to correlate the spectral features with respect to adsorption configurations of water on Pt, Pd and Au electrode surfaces, their optimized structures were computed with density functional calculations, which agree with our experimental results. The above preliminary result has shown that the first observation of SERS of water allows us to scrutinize the interfacial structure of water on the TM surfaces, providing excellent opportunities for a deeper interpretation on surface structures of water at the molecular level.[126]

In summary of this section, we have successfully prepared Au@TM nanoparticles with ideally pinhole free ultra-thin shells of various TMs, such as Pt, Pd, Co and Ni, with controllable thickness through a simple chemical method. It has been proven that the borrowing SERS activity strategy based on the core–shell nanostructures is especially useful for greatly boosting the SERS activity of TMs. Fig. 14 gives a comparison of surface enhancements of three types of SERS substrate, *i.e.*, the traditional SERS substrates (Ag, Au and Cu), pure

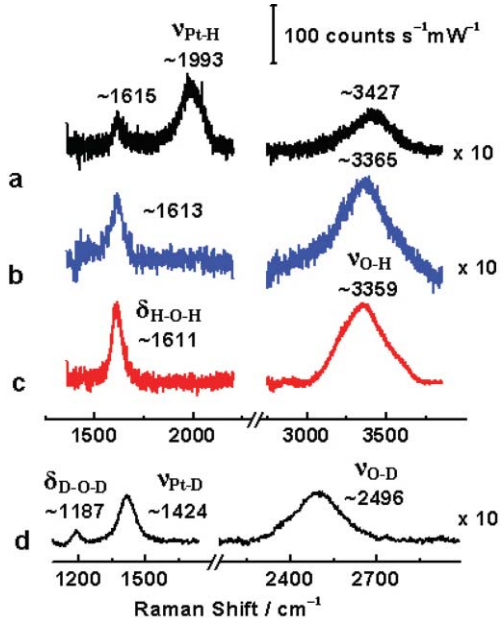

Fig. 13 SER spectra of water and deuterated water obtained on different metal surfaces in 0.1 M $NaClO_4$ at −1.6 V: (a) Pt in H_2O; (b) Pd in H_2O; (c) Au in H_2O; (d) Pt in D_2O. All the spectra have been subtracted with those obtained at +1.0 V as background; δ: bending, ν: stretching. Laser wavelength: 632.8 nm.

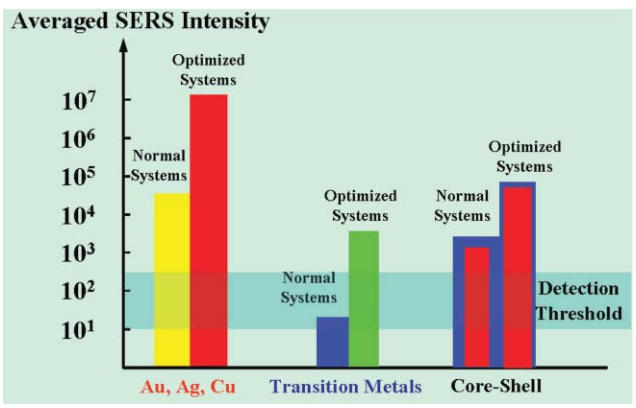

Fig. 14 A schematic illustration of the averaged enhancement factors obtained from different types of SERS substrates: Au, Ag and Cu, transition metals, and core–shell nanoparticles. The detection threshold of surface Raman spectroscopy is also given to demonstrate the importance of improving the SERS activity of the substrate.

TM substrates, and core–shell nanoparticles assembled substrate, related to the detection threshold of surface Raman spectroscopy. Among the three substrate categories, Au, Ag and Cu, as the typical SERS-active substrates, show the highest enhancement. The averaged enhancement factor can reach 10^7 when optimization is made on the size, shape and inter-particle space of aggregated nanoparticles. In the non-optimized systems, such as electrochemically roughened electrode surfaces, the surface nanostructure is random and disordered and has a very broad size distribution. Such ill-defined surfaces can only exhibit enhancement factors of about 10^5. By effectively borrowing the SERS activity from the highly active core (or substrate) of Au or Ag, the originally small surface enhancement of the TMs can be boosted by two orders of magnitude, and the total enhancement factor can approach the same level as the conventional SERS-active substrates. This indicates that, although the spectral quality may not be the same, the scope of probed molecules for the TMs could be as wide as that of Au, Ag and Cu metals, which is essentially important for developing Raman spectroscopy as a powerful tool in surface science.

Expanding surface and substrate generalities by tip-enhanced Raman spectroscopy

In the above sections, we have demonstrated the Raman signal for surface species on TMs can be significantly enhanced by using Au@TM nanoparticles borrowing the SERS activity of the Au core. The enhancement can even allow the detection of molecules with very small Raman cross sections, such as water, on TMs, which may allow the detection of practically all molecular systems. We have also pointed out that it is very important to design a SERS substrate to allow an effective coupling among the nanoparticles. Indeed, it is widely accepted that nanoparticle dimers connected by a probing molecule are the ideal configuration for generating the most effective SERS enhancement.[97,127–129] In such a dimer system, the most enhanced field appears at the junction of the two nanoparticles, which has now been conceived as the "hotspot" in single-molecular SERS.[97,127–129] Considering the importance of the junction or gap in SERS systems, and if the two nanoparticles are changed to one nanometer-sized tip and a flat substrate, we may expect also a high SERS enhancement inside the gap of them. Such a configuration is behind the concept of tip-enhanced Raman spectroscopy (TERS).[83–86]

As shown in Fig. 4, TERS borrows the enhanced electromagnetic field of the tip to boost the Raman signal of the molecules on the sample surface. The highest enhancement reported experimentally was as high as 10^6.[88a] Due to the highly localized electromagnetic field enhancement, TERS can also provide very high spatial resolution smaller than the size of tip apex, determined by the tip geometry.[100,130–132] The experimentally reported spatial resolution is as high as 14 nm,[87,133] which is much better than that of optical microscopy. The combination of high spatial resolution of SPM with the rich chemical information of Raman spectroscopy makes TERS a very promising technique for investigating processes at metal/vacuum, metal/gas and metal/electrolyte interfaces as well as in bio-related systems.

It should be pointed out that, different from the contribution of multiple SERS-active sites to SERS, the enhancement in TERS is mainly contributed by the tip as a single nanoparticle and only one "active site" (the gap between the tip and sample) is present. As a result, TERS may give a weaker signal than SERS under a similar enhancement as the number of molecules detected in TERS is roughly about 2500-fold less than that in SERS considering the difference in probing area.[134] It becomes especially difficult if one is going to study processes on well-defined single crystal surfaces, on which no or an extremely weak SERS effect exists. Therefore, it is very important to obtain a TERS tip with very high enhancement and to choose a suitable substrate to provide excellent coupling between the tip and the substrate in order to achieve an optimal TERS signal.

Electrochemical preparation of gold tips for STM-based TERS

In TERS, the enhancement is mainly provided by the tip, therefore, a metallic tip with suitable optical and chemical properties is vitally important to TERS. In our opinion, there are four very basic requirements on a TERS tip: a sharp tip apex for SPM measurement to obtain the high quality morphological image of the sample, ideal size and shape for producing prominent field enhancement, a smooth surface at the illuminated area of the tip to exclude the contribution of SERS, and free of contamination to suppress any possible background signal.

Depending on the scanning probe microscopy used for TERS, the TERS tip can be a metallic STM (scanning tunneling microscopy) tip or metal-coated AFM (atomic microscopic) tip. It is a common practice to use vacuum deposition or chemical reaction method to deposit silver or gold over commercially available AFM tips.[83–85,135] However, it is very difficult to produce TERS tips with controllable morphology and particle size at the tip apex. There were also some reports on fabricating silver STM tips for TERS, however, it is extremely difficult to obtain a very sharp end without using other ion- or electron-based sharpening techniques.[86,87] In 2004, we proposed a method to obtain very smooth and sharp gold tips used successfully for obtaining TERS.[136] Following our recipe, some other groups made further improvement.[137–139] However, the reported results were still far from satisfactory.

Aiming at the above mentioned requirements on a TERS tip, we have developed and refined the method used in our previous paper to obtain ideal Au tips for TERS.[140] Au tips can be reproducibly obtained by etching a gold wire with a diameter of 0.25 mm in a mixture of fuming HCl and absolute ethanol with a volume ratio of 1 : 1 at 2.2 V (dc) using a potentiostat to control the potential and monitor the current response. By recording the current during the etching process, it is interesting to obtain the current oscillation curve shown in Fig. 15(a). For clarity, the last 10 s of the curve was expanded and shown as the inset, from which we can clearly observe a very periodic current oscillation until the termination of the etching process. The ending point was signaled when the current reaches a preset value (normally half of the lowest current) and the electric circuit was cut-off. Using such a

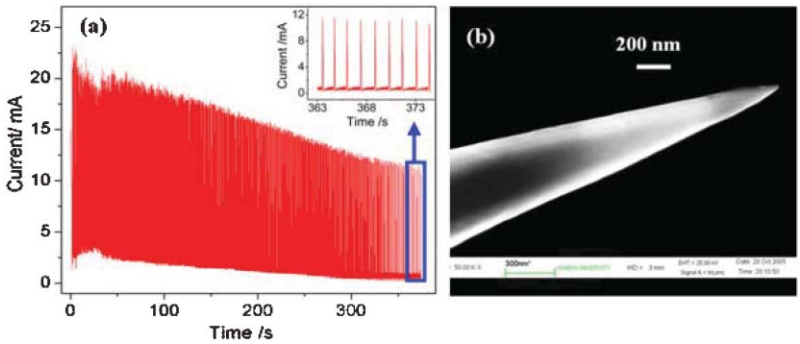

Fig. 15 (a) The current–time curve recorded during the etching process of an Au wire in a mixture of fuming HCl and ethanol solution, showing an electrochemical current oscillation. The last 10 s current response was expanded and shown as inset for clarity. (b) An SEM image of the Au tip etched in the above solution with termination control.

method, one can reproducibly fabricate Au tips with radii less than 20 nm. A typical SEM image of the tip is shown in Fig. 15(b), the tip radius is only about 12 nm. After a systematic study, we found an interesting correlation between the tip quality and current curve: a nice tip is usually accompanied by a periodic current oscillation curve. As can be seen from the figure, the surface of the tip is very smooth with extremely weak SERS activity, which can effectively minimize the possible interference of the adsorbed impurities on the tip to the TERS signal. Such a nanometer scale tip apex can provide high SERS activity and found to show very good TERS activity, which enables the observation of monolayer species adsorbed on single crystal surfaces as will be shown below.

TERS investigation of a resonant adsorbate on single crystal surfaces

After the first report in 2000, TERS has found a wide application. However, in about six years after the discovery of TERS, there are still only a few attempts to investigate adsorbed surface species, indicating the difficulty in carrying out this type of study.

The first attempt to obtain TERS signals from adsorbed species on metal surfaces can be traced back to 2000, when the Pettinger group reported the first TERS spectra of adsorbed Brilliant Cresyl Blue (BCB), a molecule with resonant Raman effect, on a smooth and semi-transparent Au film using a Ag tip.[86,141] An enhancement of up to 1500 for such a combination has been reported. The attempt to study a non-resonant Raman system is very difficult with such a low enhancement over the very small amount of molecules in the sampling region of TERS. However, if a SERS substrate, *e.g.* a rough Au film, was used, the TERS enhancement was observed for a molecule with relatively small Raman cross section, such as CN^-.[141,142] CN^- is a molecule that shows distinct Raman features on Ag and Au, which can be used as a probe to distinguish whether the signal is from the Ag tip or the Au substrate and to demonstrate whether the observed Raman signal is really from the substrate rather than from the tip contaminated in the TERS measurement.

These early studies have demonstrated that TERS can be used to investigate both smooth and rough substrates, which have expanded to some extent the surface generality of Raman spectroscopy. However, the surface structure of either the smooth Au film or rough Au substrate is far from well-defined. Therefore, the existence of SERS-active spots on the substrate may complicate the TERS response or even lead to an underestimation of the TERS enhancement. If the TERS study can be performed on well-defined atomically smooth single crystal surfaces, one may be able to use the surface selection rule to determine the surface bonding and orientation of surface species, and therefore understand the surface process unambiguously.[88]

With our long-term interest in seeking methods to obtain surface Raman signals of adsorbed species from single crystal surfaces, we carried out a collaborative work with the Pettinger group. The use of single crystal surfaces on one hand provides a good opportunity to understand the surface process with well-defined surface structure and to compare with the results obtained with other surface techniques as well as providing an ideal condition for employing surface selection rules to understand the surface Raman processes.[88] On the other hand, a defect-free surface eliminates the possible complication of SERS effect on the TERS signal and will enable a relatively accurate estimation of TERS enhancement based on the observed TERS signal with the negligible SERS enhancement from the Au(111) substrate itself.

For this purpose, we chose a molecule with resonant Raman effect that allows us to directly detect the surface Raman signal of the molecule adsorbed on well-defined single crystal surfaces. Malachite Green Isothiocyanate (MGITC) was chosen as such a probe molecule.[88] On one hand, it has an absorption peak at 629 nm, which is in almost ideal resonance with the exciting laser line of 632.8 nm. On the other hand, the molecule has an isothiocyanate group and the exposed S end can be used to bind strongly on the Au surface, which is in favor of forming a monolayer species.

A monolayer of MGITC on Au(111) surface can be routinely prepared by a drop-casting or dipping method with a MGITC ethanolic solution. Then, the electrode was rinsed with copious amount of ethanol to remove the physisorbed MGITC. Enhanced by the resonant Raman effect, the surface Raman signal of a monolayer of MGITC over a well-defined Au(111) surface can be detected with a confocal Raman instrument, and the spectrum is presented in Fig. 16(a). It is

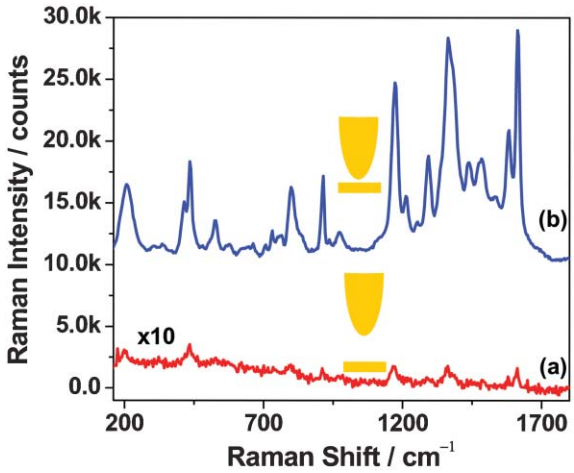

Fig. 16 Surface Raman spectra of MGITC before (a) and after (b) the approaching of the Au tip. The acquisition time was 30 s for curve (a) and 10 s for curve (b). Note that curve (a) has been enlarged by 10-fold. The laser power on the sample was 5 mW with 632.8 nm exciting line.

interesting to note that the very strong fluorescence signal detected when MGITC was dispersed over a quartz plate, was almost completely quenched when MGITC was adsorbed on Au(111) as a result of an energy transfer from MGITC to the conductive Au surface. The quenching of the strong fluorescence enables the weak surface Raman signal to be observable. The very weak surface resonance Raman (SRR) signal of MGITC becomes prominent when the Au tip was brought into tunneling region, with a gap of about 1 nm between the electrode and the substrate. This signal can be convincingly attributed to the tip-enhanced Raman signal, rather than the SERS of MGITC adsorbed on the Au tip, which has been verified by illuminating the laser directly on the tip or reexamining the tip with a Au substrate free of MGITC molecules. Although we did not find noticeable differences in the vibrational frequency in the two cases (TERS and SRR), we did observe a quite significant difference in the relative intensities, especially for the bands located below and above 1000 cm^{-1}, which may be related to the difference in the enhancement mechanism of SRR and TERS.

With both the SRR and TERS signal of MGITC, we estimate the TERS enhancement due to the existence of the Au tip. There are several methods that can be used to estimate the enhancement.[88,141,143] The first and most simple approach is the calculate the contribution of each molecule to the total Raman signal taking into account the different effective area in two techniques according to the following relation:[141]

$$G = (I_{\mathrm{TERS}}/N_{\mathrm{TERS}})/(I_{\mathrm{SRR}}/N_{\mathrm{SRR}}) \approx (I_{\mathrm{TERS}}/r^2_{\mathrm{TERS}})/(I_{\mathrm{SRR}}/r^2_{\mathrm{SRR}})$$

Several experimental results and theoretical calculations have shown that the enhanced field will be localized to a region equal to or smaller than the size of the tip apex.[100,130–132] Therefore, if we consider that the tip radius is about 20 nm in the TERS measurement and the radius of the laser spot is about 1000 nm in the SRR measurement, and that the SRR signal is about 1.3 cps and the TERS signal is over 1600 cps with this specific tip, we can estimate G to be about 3×10^6. This enhancement is comparable to that of SERS, but produces a weaker signal than SERS due to the much lower amount of molecules measured by TERS. However, such a high enhancement can only be achieved with a proper selection of the tip and the substrate, *e.g.*, Au tip and Au substrate in the present case.

The second approach to estimate the G value in TERS is based on the measurement of time constant of the photobleaching process of a dye molecule, as described in ref. 143. Photobleaching is a result of the decomposition of the molecules under the radiation of the incident light and the time constant is inversely proportional to the local field intensity of the incident light. Therefore, the TERS enhancement can be estimated by:[88,143]

$$G = (I_{\mathrm{L_{TERS}}}/I_{\mathrm{L_{SRR}}})^2 = (\tau_{\mathrm{SRR}}/\tau_{\mathrm{TERS}})^2$$

This method will sometimes be complicated by the difficulty in obtaining of a reliable τ_{SRR} and τ_{TERS} as the signal is just above the noise level in SRR, whereas the TERS signal decays very rapidly. Based on the same system, the Pettinger group recently further demonstrated that it is possible to obtain the TERS signal from several molecules with the help of resonant Raman effect.[134]

TERS investigation of non-resonant adsorbate on single crystal surfaces

The enhancement of six orders of magnitude provides an opportunity to investigate molecules without resonant Raman effect. To demonstrate this possibility, we selected benzenethiol, a molecule which does not absorb in the visible region, as a probe molecule.[88] Therefore it will not produce a resonant Raman effect using 632.8 nm excitation. Benzenethiol can easily form a monolayer on Au by cleaving the S–H bond in C_6H_5S–H to form C_6H_5S–Au. As expected, without resonant Raman effect, we have not been able to observe any Raman signal from such a monolayer species under the present experimental condition, see Fig. 17(a). However, when the tip is brought to the tunneling region, boosted by the enhancement produced by the tip, the Raman signal of the adsorbed monolayer species can be clearly observed, with a maximum intensity of 63 cps for the 1581 cm^{-1} peak, see Fig. 17(b). As we have not detected any signal of benzenethiol on Au(111) directly, we can not estimate the enhancement from the experimental result. However, if we consider a similar enhancement of 10^6 as in the case of MGITC, we may expect a surface Raman signal of only about 0.15 cps for benzenethiol on Au(111). This intensity is far below the detection threshold of the present Raman instrument. However, by borrowing the field enhancement of the Au tip, this originally very weak surface Raman signal can now be readily detected.

Since we have now been able to obtain the TERS signal from an Au(111) surface of resonant and non-resonant molecules, can we obtain the TERS signal from other TM single crystal surfaces, so that the substrate generality of Raman spectroscopy can also be extended? For this purpose, we used Pt(110) as the substrate. Similarly, we could not detect any signal of benzenethiol directly from Pt. However, when the

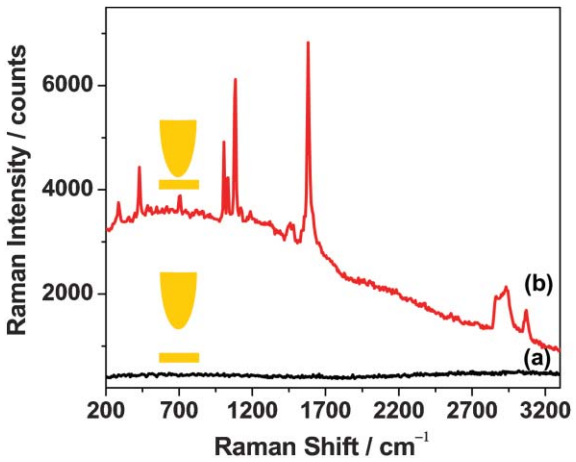

Fig. 17 Surface Raman spectra obtained on Au(111) (a) before and (b) after the approach of the Au tip. The exciting laser line was 632.8 nm. The laser power on the sample was 0.5 mW. Integration time was 60 s.

tip approached the substrate, we observed the signal from adsorbed benzenethiol on Pt, shown in Fig. 18(a). In comparison with the spectrum (Fig. 18(b)) obtained in the control experiment conducted on Au(110) using the same tip, we did observe some differences in the spectral feature (shown in Fig. 18(b), for clarity, the spectral range of 800 to 1250 cm^{-1} was expanded and shown as the inset): first, the signal intensity obtained on Pt(110) is about 20-fold weaker than that on Au(110); second, the band appearing at 1068 cm^{-1} on Pt(110) shifts to 1075 cm^{-1} on Au(110); Third, the relative height of the bands at 1075 to 1005 cm^{-1} is about twice on Au compared with that on Pt; fourth, the band width of the 1068 cm^{-1} band (*ca.* 24 cm^{-1}) on Pt is about twice than that on Au (12 cm^{-1}). The latter two factors result in a similar integrated intensity of the two bands, but with very different spectral features.

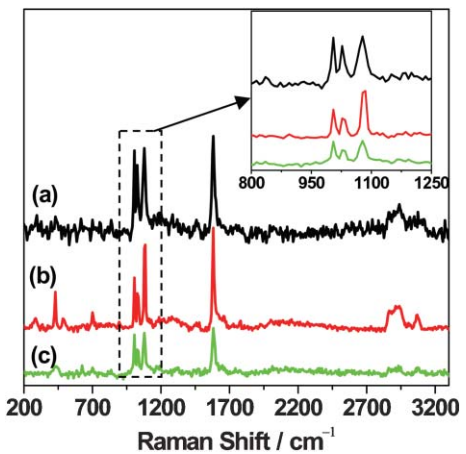

Fig. 18 TER spectra of benzenethiol adsorbed on different substrates using the same Au tip: (a) Pt(110); (b) Au(110) after the measurement of (a); (c) Pt(110) after the measurement of (b). The exciting laser line was 632.8 nm. The laser power on the sample was 5 mW except in (b), where 0.5 mW was used. All the spectra have been background subtracted.

The different spectral features of benzenethiol on Pt and Au may be due to the different interaction of this molecule with the two metal surfaces as in the case of pyridine,[144] which further demonstrates that the observed signal is from the molecule adsorbed on the substrate rather than the SERS of the molecule picked up by the tip. Actually in the above case, if we did the experiment with the same tip again on Pt(110), we observed again the same spectral feature (Fig. 18(c)), which convincingly demonstrates that the signal is really from the substrate, rather than from the tip. This result further demonstrates that TERS can be a sensitive diagnostic tool for determining the interaction of molecules with different substrates, which provides a promising opportunity to surface scientists for investigating other systems that are of great significance in practical application and fundamental research. The 20-fold difference in TERS intensity on the Au(110) and Pt(110) surfaces reveals that besides the dominant role of the tip, a suitable substrate is also vitally important to allow an optimal coupling between the tip and substrate to produce the desired SPR frequency and intensity for producing optimal TERS.

Theoretical simulation of field enhancement in TERS

In order to understand the TERS mechanism and estimate the TERS enhancement, various theoretical methods, including BEM, MMP, FEM, FDTD, have been used to obtain the field enhancement and distribution around the tip–substrate system.[100,130–132,145–148] The effect of the tip and substrate material, the incident configuration of laser, and the tip and substrate distance on the TERS enhancement has been systematically studied. Depending on the system studied, enhancements of as high as six to nine orders of magnitude have been obtained. In order to understand our experimental finding, a preliminary FDTD calculation based on the experimental conditions was performed. Au tips were modeled using a radius of 20 nm and a height of 100 nm, and the substrate and tip separation was 1 nm similar to the STM working condition. Au and Pt plates were used to simulate the Au(110) and Pt(110) surfaces. The laser is illuminated at angle of 60° to the surface normal. The yee cell size used in the present experiment is 0.5 nm × 0.5 nm × 0.5 nm, and the total number of steps is 15 000.

The calculation result was shown in Fig. 19. It can be seen from Fig. 19(a) that the highest field enhancement is about 308 when a Au substrate is used, which amounts to a Raman enhancement of 9×10^9, while for the Pt substrate the highest field enhancement is about 200, amounting to a Raman enhancement of 1.6×10^9, see Fig. 19(b). Taking account of the average effect, the Raman enhancement can still be as high as 4.5×10^8 and 8×10^7 for Au and Pt substrates, respectively. The enhancement factors are still about two orders of magnitude higher than that of the experimental result. The deviation may be due to the fact that the tip is still not of perfect round structure at the tip apex and the coupling of the laser with tip and sample is still not perfect. However, this calculation does predict that the combination of Au tip and Au substrate gives better coupling than that of Au tip and Pt substrate, as has been observed experimentally. Sectioning

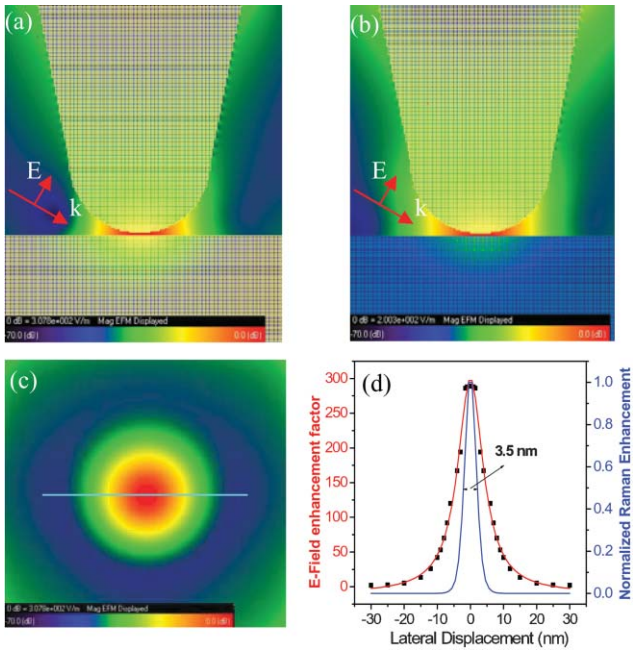

Fig. 19 FDTD calculation of the field distribution for the combination of Au tip and Au (a, c, d) and Pt (b) substrates: (a) Au tip and Au substrate; (b) Au tip and Pt substrate; (c) field distribution in the plane 0.5 nm above the substrate; (d) the line profile of the electric field enhancement and normalized Raman enhancement for the line indicated in (c). The incident direction and polarization of the laser is indicated in the figure. The tip radius is 20 nm placed 1 nm above the substrate.

the field distribution inside the gap between the Au tip and the Au substrate (Fig. 19(a)) with a plane parallel to and 0.5 nm above the substrate, we obtained Fig. 19(c), which clearly indicates that the center of the area underneath the tip apex gives the highest enhancement. To see clearly the spatial resolution that can be achieved, we plotted the *E*-field enhancement along the line indicated in Fig. 19(c) relative to the displacement to the center of the area. For clarity, the Raman enhancement is also given. As can be seen from Fig. 19(d) that the best spatial resolution of *ca.* 3.5 nm can be achieved with a 20-nm Au tip placed 1 nm above a Au substrate. Up to now, the experimentally observed best spatial resolution is about 14 nm. Apparently, there are still opportunities to further improve the spatial resolution experimentally.

Theoretical calculation by Nottinger showed that when the substrate is changed to glass the highest enhancement can only be 10^5.[130] It is therefore important to choose an appropriate tip and sample material in order to achieve the highest enhancement. Even for the cases that are not in the optimized tip and sample configuration, there are still some successful studies by dispersing samples over glass slides, *e.g.*, carbon nanotubes, quantum dots, dye molecules and more recently cell membranes using either Au or Ag tips,[83,87,149–153] showing a promising future of TERS for studying bio- and nano-related system. In summary, by borrowing the enhancement from the TERS tip, we have been able to study the adsorbed species on both rough and smooth surfaces, and on atomic flat noble-metal and TM single crystal substrates, which greatly expand both the surface generality and substrate generality of Raman spectroscopy.

Outlook and summary

As has been shown in the above two sections our group has expanded substrate, surface and molecule generalities of surface Raman spectroscopy by constructing special nanostructures, *e.g.*, SERS-active cores coated with transition-metal shells by chemical method, and SERS-active tip closely adjacent to a smooth surface by STM. In fact, with the development of nanotechnology and instrumentation, many new opportunities have been and will emerge to apply the borrowing SERS-activity strategy in various ways since 2000.[78,79,88,105,134,154–159]

The borrowing strategy has been applied to some materials and will be applied to a broad scope of materials of practical and fundamental importance, including semiconductors, polymers and dielectric materials, as illustrated in Fig. 20. Dai and co-workers[159*a*] employed the surface sol–gel (SSG) process originally developed by Kunitake and co-workers[159*b*] to allow a solution based atomic layer deposition of a TiO_2 film over a large substrate area of SERS-active silver film, see Fig. 20(a). This chemical method can overcome the drawback of relatively uncontrollable thickness in the previous sputtering or vapor deposition method. Although the enhancement is slightly decreased with the increase in the thickness, such prepared substrates show much better stability over time. The SSG method is a promising method for further expanding the substrate generality especially for materials science.

Very recently, a seminal progress has been made by Van Duyne and co-workers with a similar concept to the above study.[154] They deposited a sub-1-nm alumina layer on silver film-over-nanosphere (AgFON) substrates by atomic layer deposition (ALD), which allows them to strictly control the thickness of the alumina layer, see Fig. 20(a). With a thin layer of alumina the SERS enhancement only suffers a minor decrease (one order decrease in signal for each 2.8 nm alumina

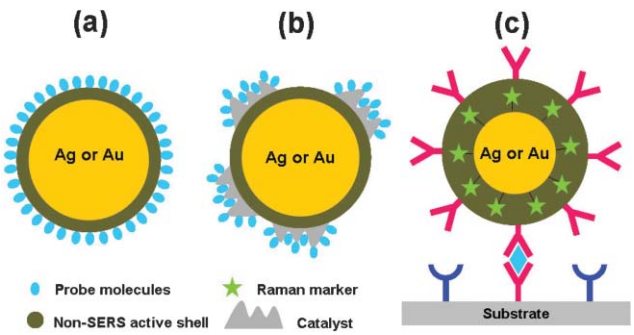

Fig. 20 Schematic illustration of three borrowing strategies using SERS-active Ag or Au cores with different shell configurations: (a) the shell is a non-SERS-active material and the target molecules are adsorbed directly on the shell surface; (b) islands of catalyst are deposited on the non-SERS-active shell surface and the target molecules are adsorbed on the catalysts; (c) the Raman marker is adsorbed directly on the core surface and the shell is modified with a group (in purple) that can bind to the target molecules (in cyan).

layer separation), therefore the SERS of AgFON substrates can be fully employed. With such substrates they have been able to achieve surface enhancement up to seven orders of magnitude, which allows them to detect species with concentration as low as 10^{-14} M.[154] It should be noted that the ultrathin ALD grown oxide layer has several important virtues: it is extremely stable to oxidation and high temperature, which helps to maintain the high stability of SERS activity and provides a very long shelf-life. Furthermore, due to the high affinity to the carboxylate groups, it is very suitable for detecting molecules with carboxylate groups on the basis of their polar interaction. After modification with catalytically active islands on the oxide layer, as illustrated in Fig. 20(b), the core–shell nanoparticles have been used to study *in-situ* catalytic processes.[154] With its ultrahigh sensitivity and stability, this method will ensure to be positioned as one of the most promising SERS methods for very wide applications.

Another conceptually different strategy is to borrow the SERS signal of a strong Raman scatterer (preferably resonant molecules) introduced as a Raman marker on the very first layer of the SERS-active nanoparticle surfaces that can be single particles or aggregates of several particles, as exemplified in Fig. 20(c). Typically the Raman-marker tagged nanoparticles were modified with glass,[155,157,158] polyelectrolyte,[160] or polymer[156] shell to provide the particle(s) with mechanical and chemical stability. The shell provides various functional groups for binding with specific molecules for further immunoassay or direct interaction with sample molecules. In this configuration, the Raman signal is not from the target molecules (or molecules to be analyzed), but from the Raman marker (or tag), therefore, it is unnecessary that the probe species should have a strong Raman signal or be in contact with the nanoparticles. This approach has been employed by several groups for multiplexed immunoassay as a very promising technique. The ultrahigh enhancement and the feasibility for multiplexed assay are two important points that this method can be used for practical application where extremely high enhancement is necessary.[156]

As mentioned above, TERS borrowing of the electromagnetic enhancement effect of the tip can be used to investigate samples without any surface enhancement effect. Therefore, it does not have a specific requirement on the surface as well as the substrate material, which allows investigation of substrates from single crystals to rough surfaces, from conductive to non-conductive substrate and greatly expands the substrate generality. However, as has been pointed out in many theoretical calculations as well as our own study, the coupling between the tip and substrate plays an important role in TERS, and will change the frequency of the localized SPR peak.[88*b*,130] Therefore, in order to achieve the highest enhancement, one has to properly choose the tip, the substrate and the excitation wavelengths.[134] In typical TERS, the enhancement is generated by the coupling of the tip with substrate, it can be considered as a single SERS cavity system. However, it may be possible in the near future to properly design and construct a multiple-tip system for investigation of sample with extremely low signal intensity. It would have great significance if TERS can work under UHV, real catalytic or electrochemical conditions, so that the surface structural effect and the chemical, catalytic or electrochemical activity can be well correlated based on well defined single crystal surfaces. The use of TERS to study cell-related systems and to sequence DNA chains with a high spatial resolution of a base are very promising and challenging directions for TERS.[149,150]

To fully employ the borrowing SERS strategy, it is necessary to further develop theoretical methods that can quantitatively account for the EM field distribution and enhancement effect. To accurately predict the enhancement for core–shell nanoparticles, it is necessary to find a theoretical method that can treat the dielectric constant for the ultrathin metallic shell. However, at present it is still not conclusive whether it is reliable to correct the dielectric constant of a bulk materials with the corrected relaxation time and effective electron mean free path by taking into account the electron and surface collision.[161,162] Furthermore, the investigation on the size-dependent dielectric constant is largely absent experimentally and theoretically, and at the present stage, most of the work has been confined to Ag and Au. The main reason is that the systematic data of the size-dependent dielectric constant related to metal nanoparticles are still unavailable and difficult to obtain experimentally. It may be possible to employ the SERS-probe molecule method to correlate the shift in the vibrational frequency of adsorbates, such as CO, with the change of the shell thickness, and thereafter to predict the electronic properties of the nanostructures theoretically.

It should be pointed out that both core–shell and TERS configurations allow the probe molecule to be isolated from the nanostructure surfaces producing a strong field enhancement. It may provide some unique systems to evaluate the contribution to SERS by the chemical enhancement that requires direct adsorbate–surface interaction. In the core–shell case, the shell thickness as the spacer can be controlled from several Å to tens of nm and material can be varied from metallic to dielectric for the systematic investigation. In the TERS case, the tip and substrate distance can be strictly controlled by SPM with air being the medium. Therefore, using both configurations and by changing the space between the molecules and the nanostructures and the material of the shell, one will be able to investigate the distance-dependent field enhancement without the complication by the chemical enhancement. Such investigation, on the other hand, will allow a systematic assessment of the contribution of chemical enhancement to SERS and ultimately for a better and comprehensive understanding of SERS mechanism(s).

Since SERS, surface-enhanced infrared spectroscopy,[36,163,164] surface-enhanced fluorescence spectroscopy[165] and surface-enhanced SFG[166] belong to a family of surface-enhanced optical spectroscopy, the borrowing strategy could be applied also in this whole family for expanding their generalities.

In summary, we have utilized two approaches to develop SERS into a more versatile and potent means with the borrowing SERS activity strategy. In the first approach, Au@TM nanoparticles have been synthesized with pinhole-free ultra-thin shells of various transition metals, such as Pt, Pd, Co and Ni, through a simple chemical reduction method. The shell thickness from about two to tens of atomic layers can

be well controlled by adjusting the ratio of the amount of the Au seed to the second metal ion in the solution. Under the optimized core size, shell thickness, inter-particle space and shell materials, the total SERS enhancement of 10^4–10^5 has been achieved by effectively borrowing the SERS activity from the highly active Au core. With such a high enhancement, we have been able to obtain the first SERS (also the first Raman) spectra of water of water/TM systems, which had been impossible using pure transition metal alone. The ability to obtain good SERS signal of water indicates that the *in-situ* vibrational properties of a great diversity of adsorbates, even with small Raman cross section, on transition metals can now be achievable by this means.

In the second approach, TERS has been employed to solve the problem of the surface generality of SERS by borrowing the enhancement from the highly SERS-active tip and also coupled enhancement from the tip. By placing an Au tip above an atomically flat Au single crystal surface, an enhancement of up to 10^6 has been obtained, which has allowed us to detect monolayer adsorbed species (resonant and non-resonant) on single-crystal metal surfaces, including Au(110), Au(111) and Pt(110), which has been considered a great challenge in surface Raman spectroscopy. To fully accomplish the borrowing strategy with various nanostructures, we have performed 3D-FDTD calculations to predict dependence of electromagnetic field enhancement on the shell thickness and/or effective distance from the highly SERS-active core, as well as the field enhancement and spatial distribution in TERS.

As a whole, the lack of substrate, surface and molecule generalities of SERS has been circumvented to some extent by these efforts. It has been shown that SERS is indeed an interesting phenomenon not only for spectroscopy and surface science but also for nanoscience because SERS-active systems must possess nanostructure and the SERS activity is critically dependent on the configuration and composition of the nanostructures.[33–44,111,167] Accordingly, there are good reasons to be optimistic that SERS will become increasingly general and indispensable tools in fundamental studies and widespread applications.

Acknowledgements

We thank NSF of China (20433040, 20473067, 20328306, 20673086), Ministry of Education of China (20040384010, NCET-05-0564) and Fok Ying Tung Foundation (101015) for funding.

References

1 C. V. Raman, *Nature*, 1928, **121**, 501.
2 *Nobel Lectures Physics, 1922–1941*, Nobel Foundation, Elsevier, Amsterdam, 1965, p. 261.
3 B. Pettinger, in *Adsorption at Electrode Surface*, ed. J. Lipkowski and P. N. Ross, VCH, New York, 1992, pp. 285.
4 R. L. McCreery, *Raman Spectroscopy for Chemical Analysis*, John Wiley, New York, 2000.
5 R. Hochleitner, N. Tarcea, G. Simon, W. Kiefer and J. Popp, *J. Raman Spectrosc.*, 2004, **35**, 515.
6 A. E. Grow, L. L. Wood, J. L. Claycomb and P. A. Thompson, *J. Microbial.. Methods*, 2003, **53**, 221.
7 G. J. Thomas, *Annu. Rev, Biophys. Biochem.*, 1999, **28**, 1.
8 L. P. Choo-Smith, H. G. M. Edwards, H. P. Endtz, J. M. Kros, F. Heule, H. Barr, J. S. Robinson, H. A. Bruining and G. J. Puppels, *Biopolymers*, 2002, **67**, 1.
9 D. A. Long, *The Raman Effect: A Unified Treatment of the Theory of Raman Scattering by Molecules*, John Wiley & Sons Ltd, Chichester, 2002.
10 (*a*) J. Behringer and J. Z. Brandmuller, *Elektrochemistry*, 1956, **60**, 643; (*b*) B. S. Galabar and T. Dudev, in *Vibrational Spectra and Structure: Vibrational Intensities*, ed. J. R. Durig, Elsevier, Amsterdam, 1996.
11 P. J. Hendra, J. R. Horder and E. J. Loader, *J. Chem. Soc. A*, 1971, 1766.
12 P. J. Hendra, I. D. M. Turner, E. J. Loader and M. Stacey, *J. Phys. Chem.*, 1974, **78**, 300.
13 T. A. Eferton and A. H. Hardin, *Catal. Rev. Sci. Eng.*, 1975, **11**, 1.
14 M. Fleischmann, P. J. Hendra and A. J. McQuillan, *Chem. Phys. Lett.*, 1974, **26**, 163.
15 (*a*) D. J. Jeanmaire and R. P. Van Duyne, *J. Electroanal. Chem.*, 1977, **84**, 1; (*b*) C. L. Haynes, C. R. Yonzon, X. Zhang and R. P. Van Duyne, *J. Raman Spectrosc.*, 2005, **36**, 471.
16 M. G. Albrecht and J. A. Creighton, *J. Am. Chem. Soc.*, 1977, **99**, 5215.
17 R. P. Van Duyne, in *Chemical and Biochemical Applications of Lasers*, ed. C. B. Moore, Academic Press, New York, 1979, vol. 4, pp. 101.
18 *Surface Enhanced Raman Scattering*, ed. R. K. Chang and T. E. Furtak, Plenum Press, New York, 1982.
19 M. Fleischmann and I. R. Hill, in *Comprehensive Treatise of Electrochemistry*, ed. R. E. White, J. O'M. Bockris, B. E. Conway and E. Yeager, Plenum Press, New York, 1984, vol. 8, p. 373.
20 M. Moskovits, *Rev. Mod. Phys.*, 1985, **57**, 783.
21 T. M. Cotton, *Adv. Spectrosc.*, 1988, **16**, 91.
22 R. L. Garrell, *Anal. Chem.*, 1989, **61**, 401A.
23 R. L. Birke, T. Lu and J. R. Lombardi, in *Techniques for Characterization of Electrodes and Electrochemical Processes*, ed. R. Varma and J. R. Selman, John Wiley & Sons, New York, 1991, p. 211.
24 A. Otto, I. Mrozek, H. Grabhorn and W. Akemann, *J. Phys.: Condens. Matter.*, 1992, **4**, 1143.
25 *Surface Enhanced Raman Vibrational Studies at Solid/Gas Interfaces, Springer Tracts in Modern Physics*, ed. I. Pockrand, Springer, New York, 1984, vol. 104.
26 A. Campion and P. Kambhampati, *Chem. Soc. Rev.*, 1998, **27**, 241.
27 R. P. Cooney, M. Fleischmann and P. J. Hendra, *J. Chem. Soc., Chem. Commun.*, 1977, 235.
28 B. Pettinger and U. Tiedemann, *J. Electroanal. Chem.*, 1987, **228**, 219.
29 M. A. Bryant, S. L. Loa and J. E. Pemberton, *Langmuir*, 1992, **8**, 753.
30 T. Maeda, Y. Sasaki, C. Horie and M. Osawa, *J. Electron Spectrosc. Relat. Phenom.*, 1993, **64/65**, 381.
31 (*a*) S. A. Bilmes, J. C. Rubim, A. Otto and A. J. Arvia, *Chem. Phys. Lett.*, 1989, **159**, 89; (*b*) C. Shannon and A. Campion, *J. Phys. Chem.*, 1988, **92**, 1385.
32 H. Yamada and Y. Yamamoto, *Surf. Sci.*, 1983, **134**, 71.
33 Z. Q. Tian, Special Issue on Surface-enhanced Raman Spectroscopy, *J. Raman Spectrosc.*, 2005, **36**, 6–7.
34 L. F. Cohen, R. Brown, M. J. T. Milton and W. E. Smith, *Faraday Discuss.*, 2006, 132.
35 K. Kneipp, M. Moskovits and H. Kneipp, Surface-enhanced Raman Scattering-Physics and Applications, *Top. Appl. Phys.*, 2006, 103.
36 *Surface-enhanced Vibrational Spectroscopy*, ed. R. Aroca, John Wiley, New York, 2006.
37 (*a*) K. Kneipp, Y. Wang, H. Kneipp, L. T. Perelman, I. Itzkan, R. R. Dasari and M. S. Feld, *Phys. Rev. Lett.*, 1997, **78**, 1667; (*b*) K. Kneipp, H. Kneipp, I. Itzkan, R. R. Dasari, M. S. Feld and M. S. Dresselhaus, *Top. Appl. Phys.*, 2002, **82**, 227.
38 (*a*) S. Nie and S. R. Emory, *Science*, 1997, **275**, 1102; (*b*) S. R. Emory and S. Nie, *J. Am. Chem. Soc.*, 1998, **120**, 8009.
39 H. X. Xu, E. J. Bjerneld, M. Kall and L. Borjesson, *Phys. Rev. Lett.*, 1999, **83**, 4357.
40 A. M. Michaels, M. Nirmal and L. E. Brus, *J. Am. Chem. Soc.*, 1999, **121**, 9932.

41 K. Kneipp, H. Kneipp, I. Itzkan, R. R. Dasari and M. S. Feld, *Chem. Rev.*, 1999, **99**, 2957; K. Kneipp, G. R. Harrison, S. R. Emory and S. Nie, *Chimia*, 1999, **53**, 35.
42 Z. Q. Tian, J. S. Gao, X. Q. Li, B. Ren, Q. J. Huang, W. B. Cai, F. M. Liu and B. W. Mao, *J. Raman Spectrosc.*, 1998, **29**, 703.
43 Z. Q. Tian, B. Ren and D. Y. Wu, *J. Phys. Chem. B*, 2002, **106**, 9463.
44 Z. Q. Tian and B. Ren, *Annu. Rev. Phys. Chem.*, 2004, **55**, 197.
45 (*a*) *Raman Microscopy*, ed. G. Turrell and J. Corset, Academic Press, San Diego, CA, 1996; (*b*) Z. Q. Tian and B. Ren, *Encyclopedia of Analytical Chemistry*, Wiley & VCH Press, Weinheim, 2000, p. 9162.
46 Z. Q. Tian, B. Ren and B. W. Mao, *J. Phys. Chem. B*, 1997, **101**, 1338.
47 B. Ren, X. F. Lin, J. W. Yan, B. W. Mao and Z. Q. Tian, *J. Phys. Chem. B*, 2003, **107**, 899.
48 P. G. Cao, J. L. Yao, B. Ren, B. W. Mao, R. A. Gu and Z. Q. Tian, *Chem. Phys. Lett.*, 2000, **316**, 1.
49 J. S. Gao and Z. Q. Tian, *Spectrochim. Acta, Part A*, 1997, **53**, 1595.
50 J. L. Yao, J. Tang, D. Y. Wu, D. M. Sun, K. H. Xue, B. Ren, B. W. Mao and Z. Q. Tian, *Surf. Sci.*, 2002, **514**, 108.
51 (*a*) W. B. Cai, B. Ren, X. Q. Li, C. X. She, F. M. Liu, X. W. Cai and Z. Q. Tian, *Surf. Sci.*, 1998, **406**, 9; (*b*) Z. Liu, Z. L. Yang, L. Cui, B. Ren and Z. Q. Tian, *J. Phys. Chem. C*, 2007, **11**, 1770; (*c*) Z. Q. Tian, B. Ren, Y. X. Chen, S. Z. Zhu and D. W. Mao, *J. Chem. Soc., Faraday Trans.*, 1996, **92**, 3829.
52 M. Moskovits, *J. Chem. Phys.*, 1978, **69**, 4159; M. Moskovits, *Top. Appl. Phys.*, 2006, **103**, 1.
53 J. Gersten and A. Nitzan, *J. Chem. Phys.*, 1980, **73**, 3023.
54 H. Metiu and P. Das, *Annu. Rev. Phys. Chem.*, 1984, **35**, 507.
55 M. Kerker, *Acc. Chem. Res.*, 1984, **17**, 271.
56 *Handbook of Vibrational Spectroscopy*, ed. G. C. Schatz and R. P. Van Duyne, Wiley, Chichester, 2002.
57 (*a*) J. H. Weaver, *Phys. Rev. B: Solid State*, 1975, **11**, 1416; (*b*) M. A. Ordal, R. J. Bell, R. W. Alexander, Jr., L. L. Long and M. R. Querry, *Appl. Opt.*, 1985, **24**, 4493.
58 B. J. Messinger, K. U. Von Raben, R. K. Chang and P. W. Baber, *Phys. Rev. B: Condens. Matter Mater. Phys.*, 1981, **24**, 649.
59 (*a*) C. L. Haynes and R. P. Van Duyne, *J. Phys. Chem. B*, 2001, **105**, 5599; (*b*) K. L. Kelly, E. Coronado, L. L. Zhao and G. C. Schatz, *J. Phys. Chem. B*, 2003, **107**, 668.
60 B. Nikoobakht and M. A. El-Sayed, *J. Phys. Chem. A*, 2003, **107**, 3372.
61 Z. Q. Tian, Z. L. Yang, B. Ren, J. F. Li, Y. Zhang, X. F. Lin, J. W. Hu and D. Y. Wu, *Faraday Discuss.*, 2006, **132**, 159.
62 J. M. Mclellan, Y. J. Xiong, M. Hu and Y. Xia, *Chem. Phys. Lett.*, 2006, **417**, 230.
63 L. Cui, F. R. Fan, Y. Zhang, Z. L. Yang, J. F. Li, B. Ren and Z. Q. Tian, unpublished work.
64 R. P. Van Duyne and J. P. Haushalter, *J. Phys. Chem.*, 1983, **87**, 2999.
65 T. M. Cotton, R. P. Van Duyne, J. C. Rubim, G. Kannen, D. Schumacher, J. Dunnwald and A. Otto, *Appl. Surf. Sci.*, 1989, **37**, 233.
66 R. P. Van Duyne, J. P. Haushalter, M. Janik-Czachor and N. Levinger, *J. Phys. Chem.*, 1985, **89**, 4055.
67 M. Fleischmann, Z. Q. Tian and L. J. Li, *J. Electroanal. Chem.*, 1987, **217**, 397.
68 G. Mengoli, M. M. Musiani, M. Fleischmann, B. W. Mao and Z. Q. Tian, *Electrochim. Acta*, 1987, **32**, 1239.
69 L. W. H. Leung and M. J. Weaver, *J. Electroanal. Chem.*, 1987, **217**, 367.
70 L. W. H. Leung and M. J. Weaver, *J. Am. Chem. Soc.*, 1987, **109**, 5113.
71 L. W. H. Leung and M. J. Weaver, *Langmuir*, 1988, **4**, 1076.
72 P. K. Aravind, A. Nitzan and H. Metiu, *Surf. Sci.*, 1981, **110**, 189.
73 A. Nitzan and L. E. Brus, *J. Chem. Phys.*, 1981, **75**, 2205.
74 C. A. Murray, D. L. Allara and M. Rhinewine, *Phys. Rev. Lett.*, 1981, **46**, 57.
75 S. Z. Zou and M. J. Weaver, *Anal. Chem.*, 1998, **70**, 2387.
76 S. Z. Zou, C. T. Williams, K.-Y. Chen Eddy and M. J. Weaver, *J. Am. Chem. Soc.*, 1998, **120**, 3811.
77 S. Z. Zou, M. J. Weaver, X. Q. Li, B. Ren and Z. Q. Tian, *J. Phys. Chem. B*, 1999, **103**, 4218.
78 M. J. Weaver, S. Z. Zou and H. Y. H. Chan, *Anal. Chem.*, 2000, **72**, 38A.
79 S. Park, P. X. Yang, P. Corredor and M. J. Weaver, *J. Am. Chem. Soc.*, 2002, **124**, 2428.
80 (*a*) A. Bruckbauer and A. Otto, *J. Raman Spectrosc.*, 1998, **29**, 665; (*b*) Y. X. Chen and A. Otto, *J. Raman Spectrosc.*, 2005, **6**(7), 736.
81 M. Futamata, *Int. J. Vib. Spectrosc.*, 2000, **2**, 9 [www.ijvs.com].
82 J. Wessel, *J. Opt. Soc. Am. B*, 1985, **2**, 1538.
83 R. M. Stöckle, Y. D. Suh, V. Deckert and R. Zenobi, *Chem. Phys. Lett.*, 2000, **318**, 131.
84 M. S. Anderson, *Appl. Phys. Lett.*, 2000, **76**, 3130.
85 N. Hayazawa, Y. Inouye, Z. Sekkat and S. Kawata, *Opt. Commun.*, 2000, **183**, 333.
86 B. Pettinger, G. Picardi, R. Schuster and G. Ertl, *Electrochemistry*, 2000, **68**, 942.
87 (*a*) N. Anderson, A. Hartschuh, S. Cronin and L. Novotny, *J. Am. Chem. Soc.*, 2005, **127**, 2533; (*b*) A. Hartschuh, E. J. Sanchez, X. S. Xie and L. Novotny, *Phys. Rev. Lett.*, 2003, **90**, 095503.
88 (*a*) B. Pettinger, B. Ren, G. Picardi, R. Schuster and G. Ertl, *Phys. Rev. Lett.*, 2004, **92**, 096101; (*b*) B. Ren, G. Picardi, B. Pettinger, R. Schuster and G. Ertl, *Angew. Chem., Int. Ed.*, 2005, **44**, 139.
89 P. K. Aravind and H. Metiu, *J. Phys. Chem.*, 1982, **86**, 5076.
90 H. X. Xu, J. Aizpurua, M. Kall and P. Apell, *Phys. Rev. E: Stat. Phys., Plasmas, Fluids, Relat. Interdiscip. Top.*, 2000, **62**, 4318.
91 J. T. Krug, II, E. J. Sanchez and X. S. Xie, *J. Chem. Phys.*, 2002, **116**, 10895.
92 M. Futamata, Y. Maruyama and M. Ishikawa, *J. Phys. Chem. B*, 2003, **107**, 7607.
93 C. Oubre and P. Nordlander, *J. Phys. Chem. B*, 2005, **109**, 10042.
94 L. J. Sherry, S. H. Chang, G. C. Schatz, R. P. Van Duyne, B. J. Wiley and Y. N. Xia, *Nano Lett.*, 2005, **5**, 2034.
95 W. H. Yang, G. C. Schztz and R. P. Van Duyne, *J. Chem. Phys.*, 1995, **103**, 869.
96 E. Hao and G. C. Schatz, *J. Chem. Phys.*, 2004, **120**, 357.
97 L. D. Qin, S. L. Zou, C. Xue, A. Atkinson, G. C. Schatz and C. A. Mirkin, *Proc. Natl. Acad. Sci. USA*, 2006, **103**, 13300.
98 J. P. Kottmann, O. J. F. Martin, D. R. Smith and S. Schultz, *Phys. Rev. B: Condens. Matter Mater. Phys.*, 2001, **64**, 235402.
99 J. P. Kottmann, O. J. F. Martin, D. R. Smith and S. Schultz, *Chem. Phys. Lett.*, 2001, **341**, 1.
100 M. Micic, N. Klymyshyn, Y. D. Suh and H. P. Lu, *J. Phys. Chem. B*, 2003, **107**, 1574.
101 P. W. Barber and S. C. Hill, *Light Scattering by Particles; Computational Methods*, World Scientific, Singapore, 1990.
102 K. S. Kunz and R. J. Luebbers, *The Finite Difference Time Domain Method for Electromagnetics*, CRC Press, LLC, Boca Raton, FL, 1993.
103 Z. P. Li, Z. L. Yang and H. X. Xu, *Phys. Rev. Lett.*, 2006, **97**, 079701.
104 J. W. Hu, Y. Zhang, J. F. Li, Z. Liu, B. Ren, S. G. Sun, Z. Q. Tian and T. Lian, *Chem. Phys. Lett.*, 2005, **408**, 354.
105 J. F. Li, Z. L. Yang, B. Ren, G. K. Liu, P. P. Fang, Y. X. Jiang, D. Y. Wu and Z. Q. Tian, *Langmuir*, 2006, **22**, 10372.
106 G. Frens, *Nat. Phys. Sci.*, 1973, **241**, 20.
107 A. Henglein, *J. Phys. Chem. B*, 2000, **104**, 2201.
108 L. H. Lu, H. S. Wang, S. Q. Xi and H. J. Zhang, *J. Mater. Chem.*, 2002, **12**, 156.
109 L. H. Lu, G. Y. Sun, H. J. Zhang, H. S. Wang, S. Q. Xi, J. Q. Hu, Z. Q. Tian and R. Chen, *J. Mater. Chem.*, 2004, **14**, 1005.
110 J. W. Hu, J. F. Li, B. Ren, D. Y. Wu, S. G. Sun and Z. Q. Tian, *J. Phys. Chem. B*, 2007, **111**, 1105.
111 M. J. Natan, *Faraday Discuss.*, 2006, **132**, 321.
112 (*a*) F. Bao, J. F. Li, J. L. Yao, B. Ren, R. A. Gu and Z. Q. Tian, unpublished work; (*b*) Z. L. Yang, PhD Thesis, Xiamen University, 2006.
113 H. Metiu, *Prog. Surf. Sci.*, 1984, **17**, 153.
114 E. J. Zeman and G. C. Schatz, *J. Phys. Chem.*, 1987, **91**, 634.
115 E. A. Coronado and G. C. Schatz, *J. Chem. Phys.*, 2003, **119**, 3926.
116 H. X. Xu, *Appl. Phys. Lett.*, 2005, **87**, 066101.
117 G. Fischer, H. Hoffmann and J. Vancea, *Phys. Rev. B: Condens. Matter*, 1980, **22**, 6065.
118 P. B. Johnson and R. W. Christy, *Phys. Rev. B: Solid State*, 1972, **6**, 4370.

119 A. M. El-Aziz, L. A. Kibler and D. M. Kolb, *Electrochem. Commun.*, 2002, **4**, 535.
120 H. Naohara, S. Ye and K. Uosaki, *J. Electroanal. Chem.*, 2001, **500**, 435.
121 (*a*) A. Henglein, *J. Phys. Chem. B*, 2000, **104**, 6683; (*b*) E. J. Zeman and G. C. Schatz, *J. Phys. Chem.*, 1987, **91**, 634.
122 M. Fleischmann, P. J. Hendra, I. R. Hill and M. E. Pemble, *J. Electroanal. Chem.*, 1981, **117**, 243.
123 Z. Q. Tian, Y. X. Chen, B. W. Mao, C. Z. Li, J. Wang and Z. F. Liu, *Chem. Phys. Lett.*, 1995, **240**, 224.
124 Y. X. Chen and Z. Q. Tian, *Chem. Phys. Lett.*, 1997, **281**, 379.
125 Y. X. Chen, S. Z. Zou, K. Q. Huang and Z. Q. Tian, *J. Raman Spectrosc.*, 1998, **29**, 749.
126 Y. X. Jiang, J. F. Li, Z. L. Yang, D. Y. Wu, B. Ren, S. Duan, J. W. Hu, Y. L. Chow and Z. Q. Tian, to be submitted.
127 S. J. Lee, A. R. Morrill and M. Moskovits, *J. Am. Chem. Soc.*, 2006, **128**, 2200.
128 K. Imura, H. Okamoto, M. K. Hossain and M. Kitajima, *Nano Lett.*, 2006, **6**, 2173.
129 T. Itoh, Y. Kikkawa, K. Yoshida, K. Hashimoto, V. Biju, M. Ishikawa and Y. Ozaki, *J. Photochem. Photobiol., A*, 2006, **183**, 322.
130 I. Notingher and A. Elfick, *J. Phys. Chem. B*, 2005, **109**, 15699.
131 A. L. Demming, F. Festy and D. Richards, *J. Chem. Phys.*, 2005, **122**, 184716.
132 W. X. Sun and Z. X. Shen, *Ultramicroscopy*, 2004, **94**, 237.
133 N. Anderson, P. Anger, A. Hartschuh and L. Novotny, *Nano Lett.*, 2006, **6**, 744.
134 K. F. Domke, D. Zhang and B. Pettinger, *J. Am. Chem. Soc.*, 2006, **128**, 14721.
135 J. J. Wang, Y. Saito, D. N. Batchelder, J. Kirkham, C. Robinson and D. A. Smith, *Appl. Phys. Lett.*, 2005, **86**, 263111.
136 B. Ren, G. Picardi and B. Pettinger, *Rev. Sci. Instrum.*, 2004, **75**, 837.
137 F. M. Huang, F. Festy and D. Richards, *Appl. Phys. Lett.*, 2005, **87**, 183101.
138 C. C. Neacsu, G. A. Steudle and M. B. Raschke, *Appl. Phys. B*, 2005, **80**, 295.
139 L. Billot, L. Berguiga, M. L. de la Chapelle, Y. Gilbert and R. Bachelot, *Eur. Phys. J.: Appl. Phys.*, 2005, **31**, 139.
140 X. Wang, Y. Cui and B. Ren, *Chem. J. Chin. Univ.*, 2007, **28**, 522.
141 B. Pettinger, G. Picardi, R. Schuster and G. Ertl, *Single Mol.*, 2002, **3**, 285.
142 B. Pettinger, G. Picardi, R. Schuster and G. Ertl, *J. Electroanal. Chem.*, 2003, **554**, 293.
143 B. Pettinger, B. Ren, G. Picardi, R. Schuster and G. Ertl, *J. Raman Spectrosc.*, 2005, **36**, 541.
144 (*a*) D. Y. Wu, B. Ren and Z. Q. Tian, *ChemPhysChem*, 2006, **7**, 619; (*b*) D. Y. Wu, B. Ren, Y. X. Jiang, X. Xu and Z. Q. Tian, *J. Phys. Chem. A*, 2002, **106**, 9042.
145 D. L. Mills, *Phys. Rev. B: Condens. Matter Mater. Phys.*, 2002, **65**, 125419.
146 S. Klein, T. Witting, K. Dickmann, P. Geshev and M. Hietschold, *Single Mol.*, 2002, **3**, 281.
147 D. S. Bulgarevich and M. Futamta, *Appl. Spectrosc.*, 2004, **58**, 757.
148 R. M. Roth, N. C. Panoiu, M. M. Adam, R. M. Osgood, C. C. Neascu and M. B. Raschke, *Opt. Express*, 2006, **14**, 2921.
149 A. Rasmussen and V. Deckert, *J. Raman Spectrosc.*, 2006, **37**, 311.
150 U. Neugebauer, P. Rçsch, M. Schmitt, J. Popp, C. Julien, A. Rasmussen, C. Budich and V. Deckert, *ChemPhysChem*, 2006, **7**, 1428.
151 T. Yano, P. Verma, S. Kawata and Y. Inouye, *Appl. Phys. Lett.*, 2006, **88**, 093125.
152 Y. Saito, M. Motohashi, N. Hayazawa, M. Iyoki and S. Kawata, *Appl. Phys. Lett.*, 2006, **88**, 143109.
153 D. H. Pan, N. Klymyshyn, D. H. Hu and H. P. Lu, *Appl. Phys. Lett.*, 2006, **88**, 093121.
154 X. Y. Zhang, J. Zhao, A. V. Whitney, J. W. Elam and R. P. Van Duyne, *J. Am. Chem. Soc.*, 2006, **128**, 10304.
155 W. E. Doering and S. Nie, *Anal. Chem.*, 2003, **75**, 6171.
156 A. F. McCabe, C. Eliasson, R. A. Prasath, A. Hernandez-Santana, L. Stevenson, I. Apple, P. A. G. Cormack, D. Graham, W. E. Smith, P. Corish, S. J. Lipscomb, E. R. Holland and P. D. Prince, *Faraday Discuss.*, 2006, **132**, 303.
157 S. P. Mulvaney, M. D. Musick, C. D. Keating and M. J. Natan, *Langmuir*, 2003, **19**, 4784.
158 J. L. Gong, J. H. Jiang, H. F. Yang, G. L. Shen, R. Q. Yu and Y. Ozaki, *Anal. Chim. Acta*, 2006, **564**, 151.
159 (*a*) L. L. Bao, S. M. Mahurin and S. Dai, *Anal. Chem.*, 2004, **76**, 4531; (*b*) J. He, I. Ichinose, T. Kunitake, A. Nakao, Y. Shiraishi and N. Toshima, *J. Am. Chem. Soc.*, 2003, **125**, 11034.
160 (*a*) K. Kim, H. K. Park and N. H. Kim, *Langmuir*, 2006, **22**, 3421; (*b*) N. H. Kim, S. J. Lee and K. Kim, *Chem. Commun.*, 2003, 724.
161 C. L. Nehl, N. K. Grady, G. P. Goodrich, F. Tam, N. J. Halas and J. H. Hafner, *Nano Lett.*, 2004, **4**, 2355.
162 V. N. Pustovit and T. V. Shahbazyan, *Phys. Rev. B: Condens. Matter Mater. Phys.*, 2006, **73**, 085408.
163 (*a*) M. Osawa, *Bull. Chem. Soc. Jpn.*, 1997, **70**, 2861; (*b*) M. Osawa, *Top. Appl. Phys.*, 2001, **81**, 163.
164 G. Q. Lu, S. G. Sun, L. R. Cai, S. P. Chen and Z. W. Tian, *Langmuir*, 2000, **16**, 778.
165 J. R. Lakowicz, C. D. Ceddes, I. Cryczynski, J. Malicka, Z. Gryczynski, K. Aslan, J. Lukomska, E. Matveeva, J. Zhang, R. Badugu and J. Huang, *J. Fluoresc.*, 2004, **14**, 425.
166 S. Baldelli, A. S. Eppler, E. Anderson, Y. R. Shen and G. A. Somorjai, *J. Chem. Phys.*, 2000, **113**, 5432.
167 (*a*) J. A. Dieringer, A. D. McFarland, N. C. Shah, D. A. Stuart, A. V. Whitney, C. R. Yonzon, M. A. Young, X. Y. Zhang and R. P. Van Duyne, *Faraday Discuss.*, 2006, **132**, 9; (*b*) J. J. Baumberg, T. A. Kelf, Y. Sugawara, S. Cintra, M. E. Abdelsalam, P. N. Bartlett and A. E. Russell, *Nano Lett.*, 2005, **5**, 2262; (*c*) S. Cintra, M. E. Abdelsalam, P. N. Bartlett, J. J. Baumberg, T. A. Kelf, Y. Sugawara and A. E. Russell, *Faraday Discuss.*, 2006, **132**, 191.

